

## Chiral symmetry and the delta-nucleon transition form factors

G. C. Gellas,<sup>1,\*</sup> T. R. Hemmert,<sup>2,†</sup> C. N. Ktorides,<sup>1</sup> and G. I. Poulis<sup>1,3,‡</sup>

<sup>1</sup>*Department of Physics, Nuclear and Particle Physics Section, University of Athens, Panepistimiopolis, GR-15771 Athens, Greece*

<sup>2</sup>*Forschungszentrum Jülich, IKP (Th.), D-52425 Jülich, Germany*

<sup>3</sup>*Institute of Accelerating Systems and Applications, Panepistimiopolis, Athens, Greece*

(Received 18 November 1998; published 6 August 1999)

The three complex form factors entering the  $\Delta \rightarrow N\gamma^*$  vertex are calculated to  $\mathcal{O}(\varepsilon^3)$  in the framework of a chiral effective theory with explicit  $\Delta(1232)$  degrees of freedom included. It is shown that the low  $q^2$  behavior of the form factors is governed by  $\pi N$ ,  $\pi\Delta$  loop effects. Predictions are given for the  $q^2$  dependence of the three transition multipoles  $M1(q^2)$ ,  $E2(q^2)$ ,  $C2(q^2)$ . Furthermore, the role of the presently unknown low energy constants that affect the values of the multipole ratios  $\text{EMR}(q^2)$  and  $\text{CMR}(q^2)$  is elucidated.

[S0556-2821(99)04215-0]

PACS number(s): 12.39.Fe, 11.30.Rd, 13.40.Hq

### I. INTRODUCTION

The electromagnetic transition of the  $\Delta(1232)$  resonance to the nucleon  $\Delta \rightarrow N\gamma^*$  is of particular interest [1–4] as far as our understanding of the structure of the latter is concerned. Historically (e.g., [5]), this reaction raised a lot of interest because it allowed one to probe the issue of whether the nucleon or its first resonance is “deformed”—the reason being that apart from the dominant magnetic dipole ( $M1$ ) transition electromagnetic selection rules also allow an electric ( $E2$ ) and a Coulomb ( $C2$ ) quadrupole transition, which vanish in simple models of the nucleon with spherical symmetry. Accordingly, the amount of deformation can be quantified by the multipole ratios  $\text{EMR}(q^2) = E2(q^2)/M1(q^2)$  and  $\text{CMR}(q^2) = C2(q^2)/M1(q^2)$ , which acquire a four-momentum (squared) dependence in the case of virtual photons  $q^2 \neq 0$ .

By the late 1990s there was a nearly uniform consensus in the physics community that indeed there exists a small quadrupole component in the electromagnetic  $N\Delta$  transition [4,6]. In the case of real photons one nowadays believes a  $\text{Re}[\text{EMR}(0)] \approx -1\% \dots -4\%$ , but a more precise determination of this fundamental property of the nucleon has been surprisingly elusive and hotly contested throughout the past decade, both among theorists and among experimentalists. It is our hope that the ongoing experiments [7] of the electroproduction of  $\Delta(1232)$  with the resulting better information on the  $q^2$  dependence of the  $N\Delta$ -transition form factors, as well as on  $\text{EMR}(q^2)$ ,  $\text{CMR}(q^2)$ , will lead to a clear picture of the underlying physics and enable us to identify the relevant degrees of freedom for several different regimes of momentum transfer. A dramatic change of the physics underlying the electromagnetic  $N\Delta$  transition is very much expected from *perturbative* QCD, which predicts for “large”  $Q^2 \equiv -q^2$  that  $\text{EMR}(Q^2) \rightarrow +1$ . At which finite  $Q^2$  the crossover from a negative to a positive EMR should happen

and whether this point is kinematically accessible at present or future electron scattering machines is a further issue of current debate and interest, e.g., [8].

From a theorist’s perspective, the treatment of the electromagnetic  $N\Delta$  transition may be grouped into two categories.

(1) Calculations of the electromagnetic  $\Delta N\gamma^*$  vertex with its associated three complex form factors *per se*, using different theoretical frameworks that aspire to fundamentally based descriptions of the  $N\Delta$  system. The chiral Bag model (e.g., [9]), quark models with meson exchange currents (e.g., [10]), lattice gauge theory (e.g., [11]), and effective chiral Lagrangians (e.g., [12,13]) constitute such attempts.

(2) Direct theoretical treatments [2,3] of the full scattering processes (e.g.,  $eN \rightarrow e'N\pi$ ,  $eN \rightarrow e'N\gamma$ ) in the  $\Delta(1232)$  resonance region, either based on phenomenological Lagrangians supplemented with a method of choice to unitarize the amplitudes or dispersion relations. A point of strong contention therein is the issue of separation of background vs resonance contributions. For a recent summary of the status of the resulting EMR and CMR extractions we refer to the talk by Workman [14].

In the present work we calculate the  $\Delta(1232)$  to  $N$  radiative transition  $\Delta \rightarrow N\gamma^*$  in the region of small (i.e.,  $Q^2 < 0.2 \text{ GeV}^2$ ) photon virtuality, utilizing a recently developed effective chiral Lagrangian approach [15,16] that systematically incorporates the spontaneous and the explicit breaking of the chiral symmetry of QCD. A small scale  $\varepsilon = \{p, m_\pi, \delta\}$  denoting, collectively, small momenta, the pion mass, and the delta-nucleon mass splitting is used to establish a systematic power counting, thus telling us precisely which diagrams and vertices have to be included if we want to calculate up to a certain order in  $\varepsilon$ . This approach allows for an efficient inclusion of a  $\Delta(1232)$  degrees of freedom consistent with the underlying chiral symmetry of QCD and is referred to as the “small scale expansion” (SSE) [15,16], constituting a phenomenological extension of heavy baryon chiral perturbation theory [17]. The formalism can be used to *calculate* both the vertex as well as full scattering amplitudes—here we focus on the former. Clearly, as we are dealing with a *low energy* effective theory, the  $q^2$  dependence of a given physical quantity can be trusted only at low

\*Email address: ggellas@atlas.cc.uoa.gr

†Email address: th.hemmert@fz-juelich.de

‡Email address: gpoulis@rtm.iasa.uoa.gr

values.<sup>1</sup> Accordingly, our final applications will be discussed in this spirit.

The most general form of the  $\Delta \rightarrow N \gamma^*$  radiative decay amplitude that complies with Lorentz covariance, gauge invariance, and parity conservation is described by three form factors. We begin our discussion from the widely used form<sup>2</sup>

$$i\mathcal{M}_{\Delta \rightarrow N \gamma}^{rel} = -\frac{e}{2M_N} \bar{u}(p_N) \gamma_5 \left[ g_1(q^2) (\not{q} \epsilon_\mu - \not{\epsilon}_\mu q) + \frac{g_2(q^2)}{2M_N} (p_N \cdot \epsilon q_\mu - p_N \cdot q \epsilon_\mu) + \frac{g_3(q^2)}{2M_N} (q \cdot \epsilon q_\mu - q^2 \epsilon_\mu) \right] u_\Delta^\mu(p_\Delta). \quad (1)$$

Here  $M_N$  is the nucleon mass,  $p_{N,\Delta}^\mu$  denotes the relativistic four-momentum of the nucleon and delta, and  $q_\mu$  and  $\epsilon_\mu$  are the photon momentum and polarization vectors, respectively. The delta is described via a Rarita-Schwinger spinor  $u_\Delta^\mu(p_\Delta)$  with free Lorentz index  $\mu$ . The  $M1$ ,  $E2$ , and  $C2$  multipoles allowed in  $\frac{3}{2}^+ \rightarrow \frac{1}{2}^+$  electromagnetic transitions can be cast as linear combinations of the form factors  $g_1$ ,  $g_2$ , and  $g_3$  [20].

In this work we study the radiative vertex to  $\mathcal{O}(\epsilon^3)$  in the above-mentioned SSE formalism. This constitutes the first order where pion-nucleon and pion-delta loop graphs enter the vertex. As will be shown later, an  $\mathcal{O}(\epsilon^3)$  calculation entails corrections up to  $\mathcal{O}(1/\Lambda_\chi^2)$ , with  $\Lambda_\chi$  the chiral symmetry breaking scale. One of the main tasks during this calculation has been the consistent matching between the results of our perturbative calculation and the most general vertex parametrization as given, for example, in Eq. (1). In order to provide for a stringent test of our new predictions with experiment we note that a complementary calculation of the full pion photoproduction amplitude in the  $\Delta(1232)$  region to the same order in  $\epsilon^3$  is in progress [21].

There have been previous analyses of the radiative transition in a similar theoretical approach by Butler *et al.* [12] and by Napsuciale and Lucio [13]. Our work differs from the aforementioned references in the following aspects.

The most crucial difference is that we address the *form factors* and not just the real-photon point. This entails (a) a  $q^2$  dependence in our expressions and (b) the presence of an additional form factor ( $g_3$ ), or, equivalently, our calculation yields the  $\text{CMR}(q^2)$ , in addition to the  $\text{EMR}(q^2)$ .

SSE systematically keeps track of  $1/M$  (i.e., relativistic) corrections to lower order couplings. These corrections have not been included in previous analyses [12,13]. We also find that our identification of the form factors differs from the one used in [13] at the real photon point.

<sup>1</sup>Similar calculations using the SSE have been performed for the electromagnetic form factors of the nucleon and good agreement with experimental data has been found in the  $Q^2 < 0.2$  GeV<sup>2</sup> regime [18,19].

<sup>2</sup>Equivalent forms, obtained via use of the equations of motion, can be found in the vast literature on this subject.

This article is structured as follows. In the next section we briefly review the essentials of the ‘‘small scale expansion’’ and its power counting. In Sec. III, we discuss the most general form of the Pauli-reduced transition amplitude which is consistent with the  $\mathcal{O}(\epsilon^3)$  calculation in the SSE. We then proceed, in Sec. IV, to calculate the loop as well as chiral counterterm contributions. The resulting expressions for the form factors are identified in Sec. V, while those for the multipoles in Sec. VI. Numerical values for the  $\text{EMR}(q^2)$ ,  $\text{CMR}(q^2)$  using presently available (theoretical) input are furnished in Sec. VII. In the same section we give numerical as well as analytical results for (complex) slopes of the three form factors. We summarize and offer our perspective for future efforts in the concluding section. Finally, we devote an appendix to the discussion of technical matters.

## II. CHIRAL LAGRANGIANS AND THE ‘‘SMALL SCALE EXPANSION’’

### A. Heavy baryon ChPT

QCD, being a strongly coupled theory at low (of the order of 1 GeV) energies, renders traditional perturbative expansions in the coupling constant inadequate. Chiral perturbation theory (ChPT) offers an alternative perturbative expansion, namely, one that is realized in terms of the external momenta involved in a given physical process. The original strategy was based on the notion that at low energies an effective theory of QCD will involve only the nearly massless (i.e., the Goldstone bosons: pions, etc.) degrees of freedom [22,23]. Accordingly, chiral perturbation theory has been very successful with respect to applications in the meson sector. With the inclusion of baryons, however, the systematic power counting of ChPT fails, since baryon masses  $M_B (\geq 1 \text{ GeV})$  cannot join the set of the expansion parameters {external momenta,  $m_\pi$ } as they are by no means small and remain finite in the chiral limit.

A systematic power counting can, nevertheless, be defined through a splitting of the nucleonic field degrees of freedom into heavy-light modes and integrating out the former. The cost of this procedure is to burden the effective description with additional, higher order contact interactions. Generalizing recent developments in heavy quark effective theories (see, e.g., [24,25]) heavy fermion methods were first applied to baryon chiral perturbation theory by Jenkins and Manohar [26]. The basic premise is the adoption of a non-relativistic mode of description, which entails a restriction to four-velocities of the form  $v_\mu \sim (1 + |\boldsymbol{\delta}|, \boldsymbol{\delta}), |\boldsymbol{\delta}| \ll 1$ . On an operational level this means that all momentum dependence in the theory is only governed by (nonrelativistic) soft momenta  $k_\mu$ , defined via

$$p_\mu = M_0 v_\mu + k_\mu, \quad (2)$$

where  $p_\mu$  is a typical nucleon relativistic four-momentum and  $M_0$  corresponds to the nucleon mass in the chiral limit. The range of validity of the resulting effective theory demands that each component  $k_\mu \ll \Lambda_\chi$ , with the chiral sym-

metry breaking scale being  $\Lambda_\chi \approx 1$  GeV. This approach is commonly referred to as heavy baryon chiral perturbation theory (HBChPT).

In the construction of the effective theory we will follow the systematics laid out in [27]. The general philosophy is to take the fully relativistic theory as the starting point and then perform a systematic nonrelativistic reduction. This procedure automatically guarantees the proper  $1/M$  corrections to the couplings in higher order Lagrangian terms. Alternatively, one could start from a general Lagrangian within the nonrelativistic framework, but then has to implement the so called ‘‘reparametrization invariance.’’ The latter approach is, for example, quite common in the field of heavy quark effective theories [28].

We now briefly sketch the derivation of the (nonrelativistic) chiral Lagrangians for matter fields. For details we refer the extensive literature of reviews (e.g., [16,17,29]).

We start from the chiral relativistic SU(2) Lagrangian for nucleons:

$$\mathcal{L}_N = \bar{\psi}_N \Gamma_N \psi_N, \quad (3)$$

with the relativistic nucleon isospinor field

$$\psi_N = \begin{pmatrix} \psi_p \\ \psi_n \end{pmatrix}$$

and

$$\Gamma_N = \Gamma_N^{(1)} + \Gamma_N^{(2)} + \dots \quad (4)$$

being a string of general nucleon-nucleon transition matrices  $\Gamma_N^{(n)}$  of increasing chiral power  $n$  [30]. For example, to leading order one obtains the well-known structure

$$\Gamma_N^{(1)} = i\mathcal{D} - M_0 + \frac{g_A}{2} \not{u} \gamma_5, \quad (5)$$

where  $\mathcal{D}_\mu$  denotes the chiral covariant derivative. The parameter  $g_A$  corresponds to the axial vector coupling constant (in the chiral limit) and the chiral tensor  $u_\mu$  describes the coupling of an odd number of pions with nucleon. For more details we refer to [30].

The second step is a redefinition of the relativistic nucleon fields via

$$\begin{aligned} N &= e^{iM_0 v \cdot x} P_v^+ \psi_N, \\ H &= e^{iM_0 v \cdot x} P_v^- \psi_N, \end{aligned} \quad (6)$$

with the velocity-dependent projection operators  $P_v^\pm = \frac{1}{2}(1 \pm \not{v})$ .  $N$  is typically called the ‘‘light’’ field, whereas  $H$  is commonly referred to as the ‘‘heavy’’ field. The relativistic Lagrangian, Eq. (3), then takes the general form

$$\mathcal{L}_N = \bar{N} \mathcal{A}_N N + (\bar{H} \mathcal{B}_N N + \text{H.c.}) - \bar{H} \mathcal{C}_N H, \quad (7)$$

where the matrices  $\mathcal{A}_N, \mathcal{B}_N, \mathcal{C}_N$  are defined via

$$\mathcal{A}_N = P_v^+ \Gamma_N P_v^+, \quad \mathcal{B}_N = P_v^- \Gamma_N P_v^+, \quad \mathcal{C}_N = P_v^- \Gamma_N P_v^-. \quad (8)$$

We note that each matrix consists of an infinite string of terms of increasing chiral power  $n$ , analogous to Eq. (4).<sup>3</sup>

Now one shifts the fields and integrates out the heavy component  $H$ . The resulting (nonrelativistic) effective Lagrangian reads

$$\mathcal{L}_N^{eff} = \bar{N} (\mathcal{A}_N + \gamma_0 \mathcal{B}_N^\dagger \gamma_0 \mathcal{C}_N^{-1} \mathcal{B}_N) N. \quad (9)$$

For the case of SU(2) the explicit form of this effective Lagrangian for spin 1/2 nucleons has been worked out up to  $n=3$  by several groups (e.g., [31,32,19]). Generalizations to even higher orders are under way [33]. The important point to note is that the inverse of matrix  $\mathcal{C}_N$  is calculated perturbatively, which confines the resulting effective Lagrangian to the nonrelativistic regime.

### B. Small scale expansion

HBChPT, as described above, has been quite successful for scattering processes off a single nucleon near threshold (for reviews see [17,34]). At higher energies, however, the contribution from nucleon resonances like  $\Delta(1232)$  can no longer be parametrized via higher order nucleon-nucleon couplings in  $\Gamma_N^{(2)}, \Gamma_N^{(3)}$ , etc. At some point, i.e., once explicit propagation of a nucleon or meson resonance has to be included, the above-described contact interaction approach breaks down. So if one is interested in kinematic conditions of such dynamic resonance contributions or in investigations into the low energy structure of nucleon resonances, it becomes mandatory to include low lying resonances as explicit degrees of freedom in the effective Lagrangian, Eq. (9). In particular this means the inclusion of the spin 3/2 nucleon resonance  $\Delta(1232)$  in the case of an SU(2) analysis.

The first efforts towards this direction were performed by Jenkins and Manohar [35]. In the present work, however, we follow a specific generalization of the construction method of Ref. [27] (as outlined above), which is called the ‘‘small scale expansion’’ [15,16,19,36,37]. The main difference to HBChPT lies in the fact that *the chiral power counting is modified in a phenomenologically inspired fashion*. In the SSE approach one expands in the small scale  $\varepsilon = \{\text{soft momenta}, m_\pi, \delta_0\}$ , where  $\delta_0 = \dot{M}_\Delta - M_0$  corresponds to the delta-nucleon mass splitting in the chiral limit, whereas in HBChPT one expands in the quantity  $p = \{\text{soft momenta}, m_\pi\}$ .<sup>4</sup> The chiral power counting of HBChPT as an expansion of all quantities in a power series

<sup>3</sup>Technically speaking, the matrices  $\mathcal{A}_N, \mathcal{B}_N$  start with chiral power  $n=1$ , while  $\mathcal{C}_N$  begins with  $n=0$ :  $\mathcal{C}_N^{(0)} = 2M_0$ . This appearance of a large mass term  $2M_0 > \Lambda_\chi$  in  $\mathcal{C}_N$  is also the reason why the  $H$  fields are denoted ‘‘heavy’’ and ultimately get integrated out.

<sup>4</sup>In strict HBChPT  $\delta_0$  counts as a quantity of order  $p^0$ . This is formally correct but can lead to poor convergence properties in the perturbation series. For more details we refer to the discussion in [37] regarding the spin polarizabilities of the nucleon.

governed by  $p^n$  is taken over by the SSE as an expansion of all quantities in a power series governed by  $\varepsilon^n$ . In the following we only briefly discuss the construction of the relevant SU(2) Lagrangians with explicit pion, nucleon, and delta degrees of freedom and their couplings to arbitrary external fields. For details we refer the interested reader to [15,16,19].

The starting point this time is a set of coupled relativistic SU(2) Lagrangians of relativistic nucleon and delta fields  $\psi_N, \psi_\mu$ :<sup>5</sup>

$$\begin{aligned}\mathcal{L}_N &= \bar{\psi}_N \Gamma_N \psi_N, \\ \mathcal{L}_\Delta &= \bar{\psi}_\mu \Gamma_\Delta^{\mu\nu} \psi_\nu, \\ \mathcal{L}_{\Delta N} &= \bar{\psi}_\mu \Gamma_{\Delta N}^\mu \psi_N + \text{H.c.},\end{aligned}\quad (10)$$

where each baryon matrix  $\Gamma_X, X=N, \Delta, \Delta N$ , is a string of terms of increasing power in  $\varepsilon^n$ , analogous to Eq. (4). For the spin 3/2, isospin 3/2 delta field we utilize a Rarita-Schwinger-isospin notation, as laid out in the Appendixes of Ref. [16]. In the Rarita-Schwinger formulation for spin 3/2 fields one encounters the well-known redundancy of degrees of freedom, which calls for six projection operators before one is able to isolate the ‘‘light’’ spin 3/2 component  $T_\mu$  from the ‘‘heavy’’ one  $G_\mu$ :

$$T_\mu = e^{iM_0 v \cdot x} P_v^+ P_{(33)\mu\nu}^{3/2} \psi^\nu, \quad (11)$$

with

$$P_{(33)\mu\nu}^{3/2} = g_{\mu\nu} - \frac{1}{3} \gamma_\mu \gamma_\nu - \frac{1}{3} (\not{k} \gamma_\mu \not{v}_\nu + \not{v}_\mu \gamma_\nu \not{k}). \quad (12)$$

The ‘‘heavy’’ spin 3/2 field  $G_\mu$  is a five-component object. An explicit representation can be found in [16] but is not needed here.

Suppressing all spin-isospin indices, the coupled set of relativistic Lagrangians in Eq. (10) can then be written as

$$\begin{aligned}\mathcal{L}_N &= \bar{N} \mathcal{A}_N N + (\bar{H} \mathcal{B}_N N + \text{H.c.}) - \bar{H} \mathcal{C}_N H, \\ \mathcal{L}_\Delta &= \bar{T} \mathcal{A}_\Delta T + (\bar{G} \mathcal{B}_\Delta T + \text{H.c.}) - \bar{G} \mathcal{C}_\Delta G, \\ \mathcal{L}_{\Delta N} &= \bar{T} \mathcal{A}_{\Delta N} N + \bar{G} \mathcal{B}_{\Delta N} N + \bar{H} \mathcal{D}_{\Delta N} T + \bar{H} \mathcal{C}_{\Delta N} G + \text{H.c.}\end{aligned}\quad (13)$$

Now one integrates out the ‘‘heavy’’ nucleon and ‘‘heavy’’ delta components  $H, G$  and finds the resulting (nonrelativistic) effective Lagrangian with explicit nucleon and delta fields:

$$\mathcal{L}_{\text{SSE}}^{\text{eff}} = \bar{T} \tilde{\mathcal{A}}_\Delta T + \bar{N} \tilde{\mathcal{A}}_N N + [\bar{T} \tilde{\mathcal{A}}_{\Delta N} N + \text{H.c.}], \quad (14)$$

with

$$\begin{aligned}\tilde{\mathcal{A}}_\Delta &= \mathcal{A}_\Delta + \gamma_0 \bar{\mathcal{D}}_{N\Delta}^\dagger \gamma_0 \bar{\mathcal{C}}_N^{-1} \bar{\mathcal{D}}_{N\Delta} + \gamma_0 \mathcal{B}_\Delta^\dagger \gamma_0 \mathcal{C}_\Delta^{-1} \mathcal{B}_\Delta, \\ \tilde{\mathcal{A}}_N &= \mathcal{A}_N + \gamma_0 \bar{\mathcal{B}}_N^\dagger \gamma_0 \bar{\mathcal{C}}_N^{-1} \bar{\mathcal{B}}_N + \gamma_0 \mathcal{B}_{\Delta N}^\dagger \gamma_0 \mathcal{C}_{\Delta N}^{-1} \mathcal{B}_{\Delta N}, \\ \tilde{\mathcal{A}}_{\Delta N} &= \mathcal{A}_{\Delta N} + \gamma_0 \bar{\mathcal{D}}_{N\Delta}^\dagger \gamma_0 \bar{\mathcal{C}}_N^{-1} \bar{\mathcal{B}}_N + \gamma_0 \mathcal{B}_\Delta^\dagger \gamma_0 \mathcal{C}_{\Delta N}^{-1} \mathcal{B}_{\Delta N}\end{aligned}\quad (15)$$

and

$$\begin{aligned}\bar{\mathcal{C}}_N &= \mathcal{C}_N - \mathcal{C}_{N\Delta} \mathcal{C}_\Delta^{-1} \gamma_0 \mathcal{C}_{N\Delta}^\dagger \gamma_0, \\ \bar{\mathcal{B}}_N &= \mathcal{B}_N + \mathcal{C}_{N\Delta} \mathcal{C}_\Delta^{-1} \mathcal{B}_{\Delta N}, \\ \bar{\mathcal{D}}_{N\Delta} &= \mathcal{D}_{N\Delta} + \mathcal{C}_{N\Delta} \mathcal{C}_\Delta^{-1} \mathcal{B}_\Delta.\end{aligned}\quad (16)$$

The explicit form of the effective Lagrangian, Eq. (14), in the SSE has been worked out to  $n=2$  in Ref. [16]. For  $n=1$  one finds

$$\begin{aligned}\tilde{\mathcal{A}}_N^{(1)} &= \mathcal{A}_N^{(1)} = i \mathbf{v} \cdot \mathbf{D} + \dot{g}_A S \cdot \mathbf{u}, \\ \tilde{\mathcal{A}}_{N\Delta}^{(1)} &= \mathcal{A}_{N\Delta}^{(1)} = \dot{g}_{\pi N\Delta} w_\mu^i, \\ \tilde{\mathcal{A}}_\Delta^{(1)} &= \mathcal{A}_\Delta^{(1)} = -(i \mathbf{v} \cdot \mathbf{D}^{ij} - \delta_0^i \xi_{3/2}^{ij} + \dot{g}_1 S \cdot u^{ij}) g_{\mu\nu}.\end{aligned}\quad (17)$$

In addition to the structures already discussed in Sec. II A one encounters the Pauli-Lubanski spin vector  $S_\mu$  and the  $\pi N\Delta, \pi\Delta\Delta$  bare coupling parameters  $\dot{g}_{\pi N\Delta}, \dot{g}_1$ . Furthermore, the chiral tensors  $w_\mu^i, u_\mu^{ij}$  parametrize the coupling of an odd number of pions to an  $N\Delta$  and a  $\Delta\Delta$  transition current, whereas  $D_\mu^{ij}$  corresponds to the chiral covariant derivative acting on a spin-3/2–isospin-3/2 field. With  $i, j=1, 2, 3$  we denote explicit isospin indices and  $\xi_{3/2}^{ij} = \frac{2}{3} \delta^{ij} - i/3 \epsilon^{ijk} \tau^k$  corresponds to the isospin 3/2 projector. For more details we refer to [16].

At  $n=2$  we are only interested in  $\Delta N\gamma$  vertices, as will be discussed in Sec. IV A. The relevant relativistic  $\mathcal{O}(\varepsilon^2)$   $\Delta N\gamma$  contact terms can be parametrized in terms of the low energy constants (LECs)  $b_1, b_6$  as follows:

$$\begin{aligned}\mathcal{L}_{\Delta N\gamma}^{(2)} &= \frac{i b_1}{4 M_0} \bar{\psi}_i^\mu [g_{\mu\nu} + y_1 \gamma_\mu \gamma_\nu] \gamma_\rho \gamma_5 f_{i+}^{\nu\rho} \psi_N \\ &\quad - \frac{b_6}{2 M_0^2} \bar{\psi}_i^\mu [g_{\mu\nu} + y_6 \gamma_\mu \gamma_\nu] \gamma_5 f_{i+}^{\nu\rho} D_\rho \psi_N + \text{H.c.},\end{aligned}\quad (18)$$

where  $f_{i+}^{\nu\rho} \equiv \frac{1}{2} \text{Tr}[f_+^{\nu\rho} \tau^i]$  denotes the isovector photon component and  $y_{1,6}$  are the so-called off-shell coupling constants.

Performing the transition to the heavy baryon fields for the vertices of interest to our calculation one finds [16]

<sup>5</sup>For notational simplicity we suppress all explicit isospin indices.



$$\tilde{A}_{N\Delta}^{(2)} = -i \frac{b_1}{2M_0} f_{+\mu\nu}^i S^\nu + \dots, \quad (19)$$

which is independent of the couplings  $y_1, b_6, y_6$ . In the radiative decay of the  $\Delta(1232)$  the fact that there is no  $S$ -wave multipole allowed precludes the possibility of having an  $\mathcal{O}(\epsilon)$   $\Delta N\gamma$  vertex. The parameter  $b_1$  therefore denotes the leading  $\gamma N\Delta$  coupling and carries the main strength of the  $M1$   $\Delta N\gamma$  transition [15,16,37].

While the desired analysis for  $n=2$  is quite simple, the situation at  $n=3$  is more complex. In fact, there is no agreement in the literature about number and/or structure of the subleading  $\Delta N\gamma$  vertices (e.g., compare Refs. [12,13,2]). In the next subsection we shall explicitly construct the  $n=3$   $\Delta N\gamma$  vertices according to the SSE approach.

### C. Construction of $\mathcal{O}(\epsilon^3)$ vertices

Referring to the SSE master formula, Eqs. (14)–(16), the relevant Lagrangian  $\mathcal{L}_{\Delta N\gamma}^{(3)}$  contains terms which have two separate origins—the dimension-6 contact interactions con-

tributing to  $A_{N\Delta}^{(3)}$  and possible  $1/M$  corrections related to the  $\mathcal{O}(\epsilon^2)$   $\Delta N\gamma$  vertices. The latter are given by

$$L_{\Delta \rightarrow N\gamma^*}^{(3)fixed} = \bar{N}(\gamma^0 \mathcal{B}_N^{\dagger(1)} \gamma^0 \mathcal{C}_N^{(0)-1} \mathcal{D}_{N\Delta}^{(2)} + \gamma_0 \mathcal{B}_{\Delta N}^{\dagger(2)} \gamma_0 \mathcal{C}_\Delta^{(0)-1} \mathcal{B}_\Delta^{(1)}) T, \quad (20)$$

where the superscripts denote the SSE dimension. The pertinent coupling matrices can be found in [16], *except* for the structures denoted as  $\mathcal{B}_{\Delta N}^{\dagger(2)}$ ,  $\mathcal{D}_{N\Delta}^{(2)}$  which only start contributing at  $\mathcal{O}(\epsilon^3)$ . We therefore construct these matrices, but only for the vertices of interest in our calculation. Using Eq. (18) and the orthogonality properties of the light-heavy projection operators [16] we find (ellipses signify terms that are irrelevant to the present analysis)

$$\mathcal{D}_{N\Delta}^{(2)} = \frac{i(b_1 + 2b_6)}{4M_0} P_- P_{(33)}^{3/2\nu\mu} \gamma_5 f_{\nu\rho}^+ \mathbf{v}^\rho + \dots \equiv \mathcal{D}_{N\Delta\gamma}^{(2)} + \dots \quad (21)$$

and (for the  $b_1$  part)

$$\mathcal{B}_{\Delta N}^{(2)b_1} = \frac{ib_1}{4M_0} \begin{bmatrix} -P_{(33)}^{3/2\nu\mu} \mathbf{v}^\rho \\ (1+3y)P_{(11)}^{1/2\mu\nu}(\gamma^\rho + \mathbf{v}^\rho) - \sqrt{3}yP_{(12)}^{1/2\mu\nu} \mathbf{v}^\rho \\ -(1+y)P_{(22)}^{1/2\mu\nu} \mathbf{v}^\rho + \sqrt{3}yP_{(21)}^{1/2\mu\nu}(\gamma^\rho + \mathbf{v}^\rho) \\ -(1+3y)P_{(11)}^{1/2\mu\nu} \mathbf{v}^\rho + \sqrt{3}yP_{(12)}^{1/2\mu\nu}(\gamma^\rho + \mathbf{v}^\rho) \\ (1+y)P_{(22)}^{1/2\mu\nu}(\gamma^\rho + \mathbf{v}^\rho) - \sqrt{3}yP_{(21)}^{1/2\mu\nu} \mathbf{v}^\rho \end{bmatrix} \gamma_5 f_{\nu\rho}^+, \quad (22)$$

where we have suppressed isospin indices. In a similar manner one obtains the contribution to  $B_{\Delta N}^{(2)}$  associated with  $b_6$ . The complete  $1/M$  corrections at  $\mathcal{O}(\epsilon^3)$  which had to be constructed via Eq. (20) then read

$$L_{\Delta \rightarrow N\gamma^*}^{(3)fixed} = \frac{b_1 + 2b_6}{4M_0^2} \bar{N}(S \cdot \tilde{D}) \mathbf{v}^\rho f_{\mu\rho}^i T_i^\mu + \frac{b_1 - 2b_6}{4M_0^2} \bar{N} f_{\rho\mu}^k \mathbf{v}^\rho \xi_{3/2}^{kj} S \cdot D^{ji} T_i^\mu + \frac{b_1}{2M_0^2} \bar{N} f_{\rho\beta}^k S^\rho \mathbf{v}^\beta \xi_{3/2}^{kj} D_\mu^{ji} T_i^\mu. \quad (23)$$

Interestingly, one observes that the off-shell couplings  $y_1, y_6$  drop out in the final result.

Finally we have to determine the dimension-6  $\gamma N\Delta$  counterterms contained in  $A_{N\Delta}^{(3)}$  as mandated by Eq. (14). Once more we have to start from that part of the most general relativistic  $\mathcal{O}(\epsilon^3)$  Lagrangian that contains all allowed  $\gamma N\Delta$  vertices at this order, in which the chiral tensor  $f_{\nu\alpha\beta}^{i+} \equiv \frac{1}{2} \text{Tr}\{\tau^i [D_\nu, f_{\alpha\beta}^+]\}$  plays a dominant part. At a first glance the following structures are possible candidates:  $g^{\mu\nu} \sigma^{\alpha\beta} \gamma_5 f_{\nu\alpha\beta}^{i+}$ ,  $g^{\mu\nu} g^{\alpha\beta} \gamma_5 f_{\nu\alpha\beta}^{i+}$ ,  $g^{\mu\alpha} \sigma^{\nu\beta} \gamma_5 f_{\nu\alpha\beta}^{i+}$ ,  $g^{\mu\alpha} g^{\nu\beta} \gamma_5 f_{\nu\alpha\beta}^{i+}$ ,  $\epsilon^{\nu\alpha\beta\mu} f_{\nu\alpha\beta}^{i+}$ , where the free index  $\mu$  is to be contracted with the corresponding index of the Rarita-Schwinger delta spinor in the initial state. It is straightforward to verify that only the first and third quantities will survive in  $A_{N\Delta}^{(3)}$  and can be shown to give identical contributions up to higher order terms. Accordingly we find

$$A_{N\Delta}^{(3)} = \frac{D_1}{4M_0^2} g^{\mu\nu} \mathbf{v}^\alpha S^\beta \frac{1}{2} \text{Tr}\{\tau^i [D_\nu, f_{\beta\alpha}^+]\} + \frac{iE_1}{2M_0} \frac{\delta_0}{M_0} f_{+\mu\nu}^i S^\nu + \dots \equiv A_{N\Delta\gamma}^{(3)} + \dots, \quad (24)$$

where  $D_1$ ,  $E_1$  are now identified as the two  $\gamma N\Delta$  low energy constants of  $\mathcal{O}(\epsilon^3)$ .<sup>6</sup> This set is sufficient for the renormalization of the process  $\Delta \rightarrow N\gamma^*$ ; a more detailed discussion of the construction of these counterterms can be found in [21].

<sup>6</sup>The second term of Eq. (24), proportional to  $E_1$ , appears in the ‘‘small scale expansion’’ due to the fact that the delta-nucleon mass splitting  $\delta_0$  counts as a quantity of  $\mathcal{O}(\epsilon)$ . Therefore one has to construct additional relativistic contact terms which are products of lower order interactions and the new small scale  $\delta_0$ . For a discussion of this issue see Ref. [19].

Gathering the above results we determine the relevant SSE  $\gamma N \Delta$  Lagrangian to  $\mathcal{O}(\epsilon^3)$ :

$$\begin{aligned} \mathcal{L}_{\Delta N \gamma}^{(3)} &= \bar{N} \mathcal{A}_{N \Delta \gamma}^{(3)} T + \bar{N} [\gamma^0 \mathcal{B}_N^{\dagger(1)} \gamma^0 (C_N^{(0)})^{-1} \mathcal{D}_{N \Delta \gamma}^{(2)} + \gamma_0 \mathcal{B}_{\Delta N \gamma}^{\dagger(2)} \gamma_0 (C_{\Delta}^{(0)})^{-1} \mathcal{B}_{\Delta}^{(1)}] T + \text{H.c.} \\ &= \frac{D_1}{4M_0^2} \bar{N} g^{\mu\nu} v^\alpha S^\beta f_{\nu\beta\alpha}^{i+} T_\mu^i + \frac{iE_1}{2M_0} \frac{\delta_0}{M_0} \bar{N} f_{+\mu\nu}^i S^\nu T_i^\mu - \frac{b_1 + 2b_6}{4M_0^2} \bar{N} (S \cdot D) v^\rho f_{\mu\rho}^{i+} T_i^\mu \\ &\quad + \frac{b_1 - 2b_6}{4M_0^2} \bar{N} f_{\rho\mu}^k v^\rho \xi_{3/2}^{kj} S \cdot D^j T_i^\mu + \frac{b_1}{2M_0^2} \bar{N} f_{\rho\beta+}^k S^\rho v^\beta \xi_{3/2}^{kj} D^j T_i^\mu + \text{H.c.} \end{aligned} \quad (25)$$

### III. NONRELATIVISTIC REDUCTION OF THE $\Delta \rightarrow N \gamma$ VERTEX

Since the leading order Lagrangian counts as  $\mathcal{O}(\epsilon)$  and, from the general exposition in the previous section, it follows that each new order in the SSE contributes a power  $\epsilon/M$ , the calculation of the radiative delta decay to  $\mathcal{O}(\epsilon^3)$  will include all terms up to  $\mathcal{O}(1/M^2)$ . Thus, in order to compare our calculation with Eq. (1) we must find the most general form of the amplitude consistent with an  $\mathcal{O}(1/M^2)$  calculation. In our case it is convenient to use the  $\Delta(1232)$  rest frame where a Pauli reduction of the amplitude allows one to identify the various multipoles.

As far as Dirac spinors are concerned the situation with the Pauli reduction is well known. For the delta field, on the other hand, we think that is worth providing our conventions. We start from a typical (e.g., [38]) Rarita-Schwinger representation of the  $\Delta(1232)$  spinor with the subsidiary conditions

$$\gamma_\mu u_\Delta^\mu = 0, \quad \partial_\mu u_\Delta^\mu = 0. \quad (26)$$

A specific representation consistent with these constraints is the following:

$$u_\Delta^\mu = \left( \frac{E_\Delta + M_\Delta}{2M_\Delta} \right)^{1/2} \begin{pmatrix} 1 \\ \boldsymbol{\sigma} \cdot \mathbf{p}_\Delta \\ E_\Delta + M_\Delta \end{pmatrix} \Sigma^\mu \chi_{3/2}, \quad (27)$$

with  $E_\Delta$ ,  $M_\Delta$ , and  $\mathbf{p}_\Delta$  the energy, mass, and three-momentum of the delta particle, respectively, and  $\Sigma^\mu$  the four-vector given by

$$\Sigma^\mu = \left[ \frac{\mathbf{S} \cdot \mathbf{p}_\Delta}{M_\Delta}, \mathbf{S} + \frac{\mathbf{S} \cdot \mathbf{p}_\Delta}{M_\Delta (E_\Delta + M_\Delta)} \mathbf{p}_\Delta \right], \quad (28)$$

where  $\mathbf{S}$  denotes the spin  $3/2 \rightarrow 1/2$  transition matrices [38].

Next, we have to expand the various terms entering Eq. (1) in powers of  $1/M$  and restrict ourselves up to  $\mathcal{O}(1/M^2)$  accuracy. Using the analogue of the four-component notation of the SSE,

$$\begin{aligned} u_\nu(r_N) &= P_\nu^+ u(p_N), \\ u_{\nu,\Delta}^\mu(r_\Delta) &= P_\nu^+ u_\Delta^\mu(p_\Delta), \end{aligned} \quad (29)$$

with  $p_X^\mu = M_0 v^\mu + r_X^\mu$ ,  $X = N, \Delta$ , we finally arrive at the following expression:

$$\begin{aligned} i\mathcal{M}_{\Delta \rightarrow N \gamma}^{(1)} &= \sqrt{\frac{2}{3}} e \bar{u}_\nu(r_N) \left\{ (S \cdot \epsilon) q_\mu \left[ \frac{g_1(q^2)}{M_N} + \mathcal{O}(1/M_N^3) \right] \right. \\ &\quad + (S \cdot q) \epsilon_\mu \left[ -\frac{g_1(q^2)}{M_N} - \frac{\delta}{2M_N^2} g_1(0) \right. \\ &\quad \left. \left. + \frac{\delta}{4M_N^2} g_2(0) + \mathcal{O}(1/M_N^3) \right] + (S \cdot q) \right. \\ &\quad \left. \times (v \cdot \epsilon) q_\mu \left[ \frac{g_1(0) - \frac{1}{2} g_2(0)}{2M_N^2} + \mathcal{O}(1/M_N^3) \right] \right. \\ &\quad \left. + (S \cdot q) (q \cdot \epsilon) q_\mu [0 + \mathcal{O}(1/M_N^3)] \right\} u_{\nu,\Delta}^\mu(0), \end{aligned} \quad (30)$$

which has been evaluated in the rest frame of the delta particle.

Some comments regarding the above equation are appropriate.

(1) To the order we are working the energy  $\omega$  of the outgoing photon four-momentum is  $\omega = M_\Delta - \sqrt{M_N^2 + \mathbf{q}^2} = \delta - \mathbf{q}^2/2M_N + \dots = \delta + \mathcal{O}(1/M_N)$ .

(2) For  $q^2=0$ , Eq. (30) is not in agreement with the analogous expression of Ref. [13]. There, the nucleon mass dependence of the Dirac spinors apparently was not taken into account.

(3) Equation (30) has been derived under the assumption that all the form factors are quantities of  $\mathcal{O}(\epsilon^0)$  at leading order.

(4) It is inconsistent with our subsequent loop results. This can be most easily seen by the structure proportional to  $\epsilon \cdot q$ . According to the  $1/M$  expansion this structure should not exist to  $\mathcal{O}(\epsilon^3)$ . However, as will turn out, the loop diagrams of Fig. 1 produce a nontrivial  $q^2$  dependence which scales as  $1/\Lambda_\chi^2 \sim 1/M^2$ .

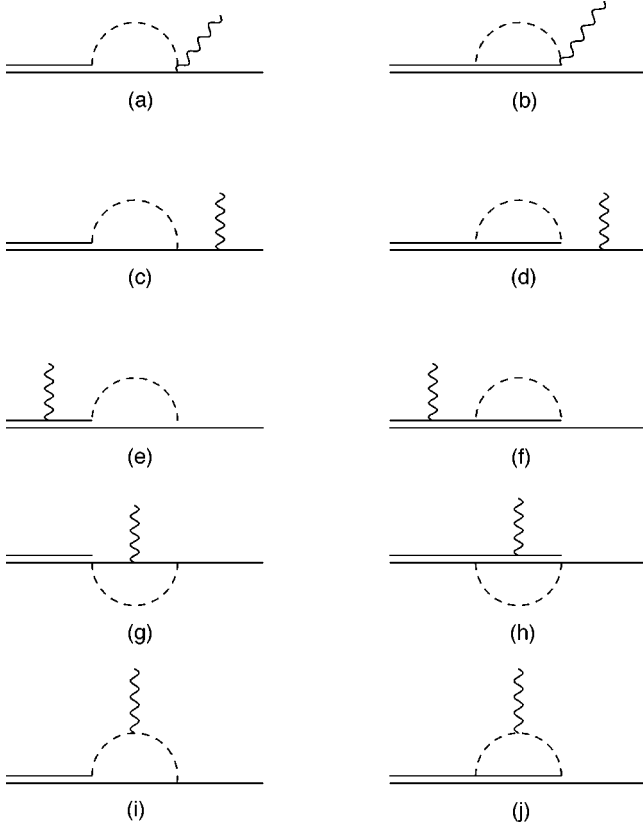


FIG. 1. Loop diagrams: single (double) solid lines denote nucleons (deltas), respectively.

We conclude that the popular form of the relativistic isovector nucleon-delta transition current, as given in Eq. (1), is not ideally suited for microscopic calculations of these form factors which rely on  $1/M$  expansions involving a chiral power counting. We find it, therefore, advantageous,<sup>7</sup> in view of the above remarks, to define a new set of form factors, by rescaling the previous ones. We propose the following definition:

$$G_1(q^2) \equiv g_1(q^2), \quad G_2(q^2) \equiv g_2(q^2),$$

$$G_3(q^2) \equiv \frac{\delta}{M_N} g_3(q^2), \quad (31)$$

which leads to the relativistic  $\Delta \rightarrow N \gamma^*$  transition matrix element

<sup>7</sup>The only alternative would be a  $g_3$  form factor which behaves as  $\mathcal{O}(\epsilon^{-1})$  at  $q^2=0$ , i.e.,  $g_3(0) \sim \Lambda_\chi/m_\pi, \Lambda_\chi/\delta$ . However, such a result would violate the basic premise of nonrelativistic formalisms like HBChPT or SSE that the large scale  $\Lambda_\chi \approx M_N, 4\pi F_\pi$  should always appear as  $\Lambda_\chi^{-n}, n \geq 0$ , in order to ensure a consistent power counting.

$$i\mathcal{M}_{\Delta \rightarrow N \gamma}^{rel} = \sqrt{\frac{2}{3}} e \bar{u}(p_N) \gamma_5 \left[ \frac{G_1(q^2)}{2M_N} (\not{q} \epsilon_\mu - \not{\epsilon} q_\mu) \right. \\ \left. + \frac{G_2(q^2)}{4M_N^2} (p_N \cdot \epsilon q_\mu - p_N \cdot q \epsilon_\mu) \right. \\ \left. + \frac{G_3(q^2)}{4M_N \delta} (q \cdot \epsilon q_\mu - q^2 \epsilon_\mu) \right] u_\Delta^\mu(p_\Delta). \quad (32)$$

Equation (32) will serve as the reference point for future comparisons with other calculations. The advantage offered by this parametrization can be seen best when performing a  $1/M$  expansion of Eq. (32), once more restricted to  $\mathcal{O}(1/M^2)$ :

$$i\mathcal{M}_{\Delta \rightarrow N \gamma}^{NR} = \sqrt{\frac{2}{3}} e \bar{u}_v(r_N) \left\{ (S \cdot \epsilon) q_\mu \left[ \frac{G_1(q^2)}{M_N} + \mathcal{O}(1/M_N^3) \right] \right. \\ \left. + (S \cdot q) \epsilon_\mu \left[ -\frac{G_1(q^2)}{M_N} - \frac{\delta G_1(0)}{2M_N^2} + \frac{\delta G_2(q^2)}{4M_N^2} \right. \right. \\ \left. \left. + \frac{q^2}{4M_N^2 \delta} G_3(q^2) + \mathcal{O}(1/M_N^3) \right] + (S \cdot q)(v \cdot \epsilon) q_\mu \right. \\ \left. \times \left[ \frac{G_1(0)}{2M_N^2} - \frac{G_2(q^2)}{4M_N^2} + \mathcal{O}(1/M_N^3) \right] + (S \cdot q)(q \cdot \epsilon) q_\mu \right. \\ \left. \times \left[ -\frac{G_3(q^2)}{4M_N^2 \delta} + \mathcal{O}(1/M_N^3) \right] \right\} u_{v,\Delta}^\mu(0). \quad (33)$$

The above formula serves as the basic connection between our (nonrelativistic) results calculated via the SSE and the desired (relativistic) transition current, Eq. (32). One can easily see that to  $\mathcal{O}(\epsilon^3)$  one is sensitive to the leading and subleading behavior of the form factor  $G_1(q^2)$ , whereas the form factors  $G_2(q^2), G_3(q^2)$  start out at  $1/M^2$  and therefore only allow us to determine them to leading order. One can also check that Eq. (33) is gauge invariant to  $\mathcal{O}(1/M^2)$  and allows for a nonvanishing  $q^2$ -dependent contribution in each of the four independent structures, consistent with the SSE calculation to  $\mathcal{O}(\epsilon^3)$ . We now move to the details of the calculation.

## IV. CALCULATION

### A. Born contributions

In the present subsection we discuss the Born contribution to the amplitude. The relevant expressions resulting from each  $\Delta N \gamma^*$  tree level vertex have the following explicit forms:<sup>8</sup>

<sup>8</sup>To the order we are working we can identify the parameters  $M_0, \delta_0$  with the physical values  $M_N, \delta = M_\Delta - M_N$ .

$$\begin{aligned}
i\mathcal{M}_{\Delta \rightarrow N\gamma^*}^{b_1} &= -\sqrt{\frac{2}{3}}e\bar{u}_v(r_N)\left[S\cdot q\epsilon_\mu\frac{b_1}{2M_N}\right. \\
&\quad \left.-S\cdot\epsilon q_\mu\frac{b_1}{2M_N}\right]u_{v,\Delta}^\mu(0), \\
i\mathcal{M}_{\Delta \rightarrow N\gamma^*}^{E_1} &= -\sqrt{\frac{2}{3}}e\bar{u}_v(r_N)\left[(S\cdot\epsilon q_\mu\right. \\
&\quad \left.-S\cdot q\epsilon_\mu)\frac{E_1\delta}{2M_N^2}\right]u_{v,\Delta}^\mu(0), \\
i\mathcal{M}_{\Delta \rightarrow N\gamma^*}^{D_1} &= -\sqrt{\frac{2}{3}}e\bar{u}_v(r_N)\left[-S\cdot\epsilon q_\mu\frac{D_1\delta}{4M_N^2}\right. \\
&\quad \left.+\epsilon_0S\cdot qq_\mu\frac{D_1}{4M_N^2}\right]u_{v,\Delta}^\mu(0), \\
i\mathcal{M}_{\Delta \rightarrow N\gamma^*}^{b_1rc} &= -\sqrt{\frac{2}{3}}e\bar{u}_v(r_N)\left[S\cdot q\epsilon_\mu\frac{b_1\delta}{4M_N^2}\right. \\
&\quad \left.+\epsilon_0S\cdot qq_\mu\frac{-b_1}{4M_N^2}\right]u_{v,\Delta}^\mu(0), \\
i\mathcal{M}_{\Delta \rightarrow N\gamma^*}^{b_6rc} &= -\sqrt{\frac{2}{3}}e\bar{u}_v(r_N)\left[S\cdot q\epsilon_\mu\frac{b_6\delta}{2M_N^2}\right. \\
&\quad \left.+\epsilon_0S\cdot qq_\mu\frac{-b_6}{2M_N^2}\right]u_{v,\Delta}^\mu(0), \tag{34}
\end{aligned}$$

where the superscripts tabulate the relevant vertices, in relation to the LECs, while ‘‘rc’’ stands for ‘‘relativistic correction.’’

We mention that the second relativistic correction Lagrangian term in Eq. (23) gives *zero* contribution to our form factors. To see this, note that the derivatives acting on the delta field bring down factors  $(S\cdot r_\Delta)$  and  $(r_\Delta\cdot T)$  where  $r_\Delta^\mu$  is the  $\Delta(1232)$  soft momentum. In the  $\Delta(1232)$  rest frame, where our calculation is performed one finds  $r_\Delta^\mu = \delta\nu^\mu$ . Both  $(S\cdot r_\Delta)$  and  $(r_\Delta\cdot T)$  therefore vanish due to the light delta constraints. We do anticipate, on the other hand, that this operator will contribute to the resonant Born diagram in pion photoproduction where the intermediate  $\Delta(1232)$  will also contain off-shell components of the delta field.

The overall Born contribution, therefore, is

$$\begin{aligned}
i\mathcal{M}_{\Delta \rightarrow N\gamma^*}^{Born} &= -\sqrt{\frac{2}{3}}e\bar{u}_v(r_N)\left[S\cdot\epsilon q_\mu\left(\frac{-b_1}{2M_N} + \frac{(2E_1 - D_1)\delta}{4M_N^2}\right)\right. \\
&\quad \left.+S\cdot q\epsilon_\mu\left(\frac{b_1}{2M_N} - \frac{E_1\delta}{2M_N^2} + \frac{(b_1 + 2b_6)\delta}{4M_N^2}\right)\right. \\
&\quad \left.+v\cdot\epsilon S\cdot qq_\mu\left(\frac{D_1}{4M_N^2} - \frac{b_1 + 2b_6}{4M_N^2}\right)\right]u_{v,\Delta}^\mu(0). \tag{35}
\end{aligned}$$

In the next subsection we will turn our attention to contributions from loop corrections to the transition vertex.

### B. Loop contributions

To  $\mathcal{O}(\varepsilon^3)$  one can draw ten independent loop diagrams for the  $\Delta \rightarrow N\gamma$  transition (see Fig. 1). However, because of the constraints  $v\cdot u_{v,\Delta}^i = S\cdot u_{v,\Delta}^i = \tau_i u_{v,\Delta}^i = 0$  satisfied by the on-shell spin 3/2 isospin 3/2 spinor  $u_{v,\Delta}^\mu$ , only diagrams 1i, 1j in Fig. 1 survive. Their contribution can be formally written as

$$\begin{aligned}
i\mathcal{M} &= -\sqrt{\frac{2}{3}}\frac{2eg_{\pi N\Delta}}{F_\pi^2}\bar{u}_v(r_N)\{(S\cdot\epsilon)q_\mu[g_A F_N + \chi g_1 F_\Delta] \\
&\quad + (S\cdot q)\epsilon_\mu[g_A G_N + \chi g_1 G_\Delta] \\
&\quad + (S\cdot q)q_\mu[\epsilon_0[g_A J_N + \chi g_1 J_\Delta] \\
&\quad + (q\cdot\epsilon)[g_A H_N + \chi g_1 H_\Delta]\}u_{v,\Delta}^\mu(0). \tag{36}
\end{aligned}$$

Here the  $N$  and  $\Delta$  labels on the functions  $F_i, G_i, \dots$  denote the intermediate baryon propagator in diagrams (i) and (j) of Fig. 1, respectively, while the isospin factor  $\chi$  takes the value  $-\frac{5}{3}$ . The loop functions are defined via

$$\begin{aligned}
F_N(t) &= 2\int_0^1 dx(x-1)\frac{A^{301}(\delta x, M_t^2)}{d}, \\
F_\Delta(t) &= 2\int_0^1 dx\left[(1-x)\frac{A^{301}(-\delta x, M_t^2)}{d}\right. \\
&\quad \left.+ 2x\frac{A^{301}(-\delta x, M_t^2)}{d(d-1)}\right], \\
G_N(t) &= 2\int_0^1 dx x\frac{A^{301}(\delta x, M_t^2)}{d}, \\
G_\Delta(t) &= -2\int_0^1 dx\left[x\frac{A^{301}(-\delta x, M_t^2)}{d}\right. \\
&\quad \left.+ 2(1-x)\frac{A^{301}(-\delta x, M_t^2)}{d(d-1)}\right], \\
J_N(t) &= \int_0^1 dx x(1-x)A^{310}(\delta x, M_t^2), \\
J_\Delta(t) &= \int_0^1 dx x(1-x)\frac{d-3}{d-1}A^{310}(-\delta x, M_t^2), \\
H_N(t) &= \int_0^1 dx x(1-x)(1-2x)A^{300}(\delta x, M_t^2), \\
H_\Delta(t) &= \int_0^1 dx x(1-x)(2x-1)\frac{d-3}{d-1}A^{300}(-\delta x, M_t^2), \tag{37}
\end{aligned}$$



where the  $t \equiv q^2$  dependence arises implicitly through  $M_t^2 = m_\pi^2 + tx(x-1)$ . Explicit representations for the  $A^{ijk}(\Omega, M_t^2)$  are given in the Appendix. The  $1/M^2$  sensitivity of our calculation is saturated by the two inverse powers of the quantity  $4\pi F_\pi \sim M$  which is of the order of the chiral symmetry breaking scale  $\Lambda_\chi (= \{4\pi F_\pi, M_N\})$ .

We close the present subsection with a brief discussion concerning renormalization issues. It is straightforward, using Eqs. (37) and (A5), to see that Eq. (36) for the loop contributions to the decay amplitude of the  $\Delta(1232)$  is a *complex* quantity and contains several divergent pieces. The lower-order couplings  $b_1, b_6$  only possess a finite part, whereas the infinities encountered in the loop amplitudes are absorbed by the infinite parts of the  $\mathcal{O}(\varepsilon^3)$  counterterms<sup>9</sup>  $E_1, D_1$ :

$$\begin{aligned} D_1 &= D_1^r(\lambda) + 16\pi^2 \beta_{D_1} L, \\ E_1 &= E_1^r(\lambda) + 16\pi^2 \beta_{E_1} L, \end{aligned} \quad (38)$$

with [19]

$$L = \frac{\lambda^{d-4}}{16\pi^2} \left[ \frac{1}{d-4} + \frac{1}{2} (\gamma_E - 1 - \ln 4\pi) \right]. \quad (39)$$

The two pertinent beta functions  $\beta_{D_1}, \beta_{E_1}$  can be found from Eq. (37) and the expressions in the Appendix. It is straightforward to obtain the results

$$\begin{aligned} \beta_{D_1} &= \frac{g_{\pi N \Delta} M_N^2}{6\pi^2 F_\pi^2} (g_A - 5/9 g_1), \\ \beta_{E_1} &= \frac{g_{\pi N \Delta} M_N^2}{6\pi^2 F_\pi^2} (g_A - 20/9 g_1). \end{aligned} \quad (40)$$

At the moment, however, we have no information about the numerical size of their finite parts  $E_1^r(\lambda), D_1^r(\lambda)$  at the chosen renormalization scale  $\lambda$ , as well as about the magnitude of the coupling  $b_6$ . We note that this information will be available in the near future as several calculations regarding different scattering processes in the delta resonance region using the SSE are underway, which will allow for a systematic extraction of the relevant higher order  $N\Delta$ -couplings. In Sec. VII we will nevertheless give some numerical estimates for linear combinations of these couplings based on calculations for  $N\Delta$ -transition multipoles performed in theoretical frameworks outside the SSE.

### C. Note on gauge invariance

Gauge invariance requires that, upon setting  $\epsilon^\mu \rightarrow q^\mu$ , the amplitude must vanish. The general amplitudes, Eqs. (30)

<sup>9</sup>The interaction terms proportional to these two LECs are what one calls counterterms in the conventional field theoretical language. Nevertheless, as is usual in ChPT, we will sometimes employ the same name for the  $b_1, b_6$  couplings.

and (33), satisfy this requirement explicitly (recall that  $\epsilon_0 \rightarrow q_0 = \delta$ ). In the case of our loop calculation this requires

$$F_i(t) + G_i(t) + \delta J_i(t) + t H_i(t) = 0, \quad (41)$$

separately for  $i=N$  and  $i=\Delta$ . This provides for a stringent test of our calculation. From the explicit formulas Eqs. (37) and (A5), one can show that the constraints of Eq. (41) are indeed satisfied. This is most easily seen by partial integration of the  $1/(\sqrt{\Omega^2 - M_t^2})$  part of  $(\delta J_i + t H_i)$ .

### V. $\Delta \rightarrow N\gamma^*$ FORM FACTORS TO $\mathcal{O}(\varepsilon^3)$

Combining the loop result, Eq. (36), with the Born contributions, Eq. (35), we obtain the total  $\mathcal{O}(\varepsilon^3)$  amplitude. This is to be compared with the general form of the amplitude, Eq. (33). The identification of the three form factors is straightforward. At this point we have no information about the magnitude of the counterterms  $b_1, b_6, D_1, E_1$ . However, the important observation is that the unknown counterterms only affect the *overall normalization* of the three form factors  $G_i(q^2)$  and leave the  $q^2$  dependence *unaffected*. We therefore separate the real photon point  $q^2=0$  from each form factor and write

$$\begin{aligned} G_1(q^2) &= G_1(0) + \tilde{g}_1(q^2), \\ G_2(q^2) &= G_2(0) + \tilde{g}_2(q^2), \\ G_3(q^2) &= G_3(0) + \tilde{g}_3(q^2), \end{aligned} \quad (42)$$

with  $\tilde{g}_i(0) \equiv 0, i=1,2,3$ . It is then straightforward to arrive at the results of Table I. Comparing the *relativistic* form of the coupling structure proportional to  $b_1$ , Eq. (18), with our general *relativistic* amplitude, Eq. (32), one expects that only the  $G_1$  form factor receives contributions from this coupling, which also holds in the nonrelativistic SSE formalism. Analogously, the coupling  $b_6$  in Table I is shown only to contribute to the form factor  $G_2$ , again as expected from its relativistic analogue in Eq. (18). Furthermore, the results of Table I are, as they should be, gauge independent. This happens automatically for the chiral counterterm contributions. For the loop contributions, however, gauge invariance can be explicitly demonstrated via the use of Eq. (41).

The results of Table I can now be compared with the ones in Ref. [13] where only the real-photon case is considered (no  $G_3$ ). We find a difference from our result originating in Eq. (30). In particular, there is no contribution to  $G_2$  from the  $b_1$  counterterm. This happens because, in [13], the coefficient of  $G_1$  in the  $(S \cdot q)(\epsilon \cdot T_3)$  term is  $2M_N$  rather than  $2M_N + \delta$ .

In Sec. VII we derive an estimate for the unknown couplings. We will then be in position to describe both the  $q^2$  dependence and the overall normalization of the three form factors. Once again we stress that *chiral symmetry demands that these form factors are complex quantities*, which is due to the on-shell  $\pi N$  intermediate state of loop diagram (i) in Fig. 1.

TABLE I. The  $\Delta N\gamma$  form factors:  $\alpha = -2g_{\pi N\Delta}M_N^2/F_\pi^2$  and  $[\mathbf{I}]$  is shorthand notation for  $[g_A I_N + \chi g_1 I_\Delta]$ , with  $I \in \{F, J, H\}$ .

Source	$G_1$	$G_2$	$G_3$
Loops	$\frac{\alpha}{M_N}[\mathbf{F}] \equiv \tilde{g}_1(q^2)$	$-4\alpha[\mathbf{J}] \equiv \tilde{g}_2(q^2)$	$-4\alpha\delta[\mathbf{H}] \equiv \tilde{g}_3(q^2)$
$\mathcal{A}_{\Delta N}^{(2)}$	$\frac{b_1}{2}$	$b_1$	0
$\gamma_0 \mathcal{B}_N^{\dagger(1)} \gamma_0 \frac{1}{C_N^{(0)}} \mathcal{D}_{N\Delta}^{(2)}$	0	$-b_1 - 2b_6$	0
$\gamma_0 \mathcal{B}_{\Delta N}^{(2)\dagger} \gamma_0 \frac{1}{C_\Delta^{(0)}} \mathcal{B}_\Delta^{(1)}$	0	0	0
$\mathcal{A}_{D_1}^{(3)}$	$\frac{\delta}{4M_N} D_1$	$D_1$	0
$\mathcal{A}_{E_1}^{(3)}$	$-\frac{\delta}{2M_N} E_1$	0	0

## VI. CONNECTION TO $\Delta \rightarrow N\gamma^*$ TRANSITION MULTIPOLES

In the relativistic case the identification of the transition multipoles  $M1(q^2)$ ,  $E2(q^2)$ ,  $C2(q^2)$  in terms of the ‘‘Dirac’’-type form factors  $G_1(q^2), G_2(q^2), G_3(q^2)$  is obtained [20] by reading off the spin-space tensor properties of the Pauli-reduced most general amplitude, Eq. (32), in the  $\mathbf{q} \cdot \boldsymbol{\epsilon} = 0$  gauge. The explicit expressions read<sup>10</sup>

$$\begin{aligned}
 M1(q^2) &= c_\Delta \left\{ G_1(q^2) [(3M_\Delta + M_N)(M_\Delta + M_N) - q^2] \right. \\
 &\quad \left. - G_2(q^2) \frac{M_\Delta}{2M_N} (M_\Delta^2 - M_N^2 - q^2) - G_3(q^2) q^2 \frac{M_\Delta}{\delta} \right\}, \\
 E2(q^2) &= -c_\Delta \left\{ G_1(q^2) (M_\Delta^2 - M_N^2 + q^2) \right. \\
 &\quad \left. - G_2(q^2) \frac{M_\Delta}{2M_N} (M_\Delta^2 - M_N^2 - q^2) - G_3(q^2) q^2 \frac{M_\Delta}{\delta} \right\}, \\
 C2(q^2) &= -c_\Delta 2M_\Delta |\vec{q}| \left\{ G_1(q^2) - G_2(q^2) \frac{E_N}{2M_N} \right. \\
 &\quad \left. - G_3(q^2) \frac{\omega}{2\delta} \right\}, \tag{43}
 \end{aligned}$$

with

$$c_\Delta = \frac{e|\vec{q}|}{12M_N M_\Delta \sqrt{2M_N(E_N + M_N)}} \sqrt{\frac{2M_\Delta}{M_\Delta^2 - M_N^2}}. \tag{44}$$

We now need to match these general expressions to the  $\mathcal{O}(1/M^2)$  accuracy of our results for the  $G_1, G_2, G_3$  form factors obtained via the SSE in the previous section. We may

proceed in two ways: (1) Use the same reasoning as in the relativistic case, i.e., obtain the multipoles from the spin tensor structure of the appropriate Pauli-reduced expression, Eq. (33); (2) expand the relativistic formulas for the multipoles to  $\mathcal{O}(1/M^2)$ .

In both cases we obtain

$$\begin{aligned}
 M1(q^2) &= \frac{e\sqrt{\delta^2 - q^2}}{6\sqrt{\delta}} \left[ \frac{2G_1(q^2)}{M_N} - \frac{\delta}{4M_N^2} G_2(q^2) \right. \\
 &\quad \left. - \frac{q^2}{4\delta M_N^2} G_3(q^2) + \mathcal{O}(1/M_N^3) \right], \\
 E2(q^2) &= \frac{e\sqrt{\delta^2 - q^2}}{6\sqrt{\delta}} \left[ -\frac{\delta}{2M_N^2} G_1(0) + \frac{\delta}{4M_N^2} G_2(q^2) \right. \\
 &\quad \left. + \frac{q^2}{4\delta M_N^2} G_3(q^2) + \mathcal{O}(1/M_N^3) \right], \\
 C2(q^2) &= \frac{e(\delta^2 - q^2)}{6\sqrt{\delta}} \left[ -\frac{1}{2M_N^2} G_1(0) + \frac{1}{4M_N^2} G_2(q^2) \right. \\
 &\quad \left. + \frac{1}{4M_N^2} G_3(q^2) + \mathcal{O}(1/M_N^3) \right]. \tag{45}
 \end{aligned}$$

From Eq. (45) one can directly see that the  $\mathcal{O}(\epsilon^3)$  prediction for  $M1$  is sensitive to subleading order, whereas the prediction for the quadrupole multipoles  $E2, C2$  only gives us the leading result. One also observes the peculiar behavior that *in the case of the  $E2, C2$  form factors their  $q^2$  dependence is not suppressed by powers of  $1/M_N$  with respect to the  $q^2 = 0$  point.* According to our knowledge this situation has not been observed<sup>11</sup> before in chiral calculations of form factors,

<sup>10</sup>At the photon point ( $q^2 = 0$ ) one easily verifies that they agree with the corresponding expressions given in [2]. We are grateful to Rick Davidson for valuable support on this point.

<sup>11</sup>The notable exception has been the pseudoscalar form factor of the nucleon which is known to be dominated by the light pion physics [19].

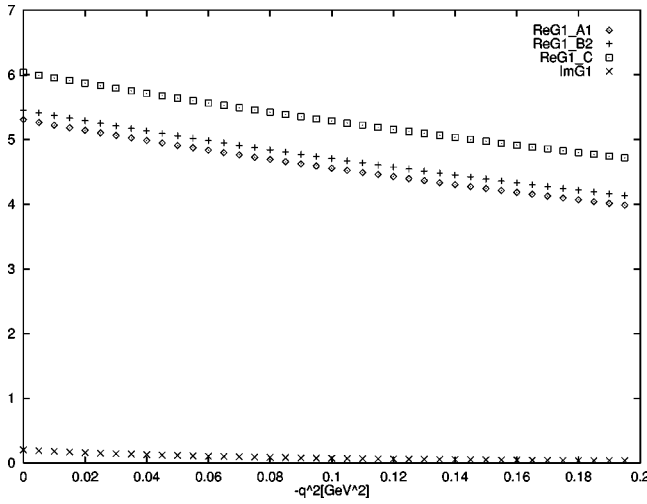


FIG. 2. The real and imaginary parts of the form factor  $G_1$  with  $C_2, C_3$  given by the sets  $A_1, B_2, C$ .

e.g., compare [17,19].<sup>12</sup> Its formal origin lies in the fact that for quadrupole transitions it is not possible to write down a counterterm at a lower order than  $\mathcal{O}(\epsilon^3)$ , i.e., the same order where loops start contributing. *Keeping the above caveat in mind, i.e. that Eq. (45) only represents the leading behavior for the E2, C2 form factors, the chiral structure underlying Eq. (45) leads us to the expectation that the E2, C2 form factors only show a weak suppression at low  $q^2$  with respect to their  $q^2=0$  point and that the  $q^2$  evolution could be very different from the corresponding (dipole behavior of the) nucleon Sachs form factors  $G_E(q^2), G_M(q^2)$ , e.g., [17,19].* On the other hand, the  $M1$  form factor shows the expected  $1/M$  suppression of its radius with respect to the photon point—quite analogous to the SSE calculation of the dipole form factor  $G_M(q^2)$  in [19]. This question will be addressed in more detail in a future communication once precision information on the relevant coupling constants is available. We further note that the quadrupole multipoles in Eq. (45) satisfy the long wavelength ( $|\mathbf{q}| \rightarrow 0$ ) constraint  $E_2 = (q_0/|\mathbf{q}|)C_2$ .

## VII. NUMERICAL RESULTS

To provide numerical results we need to fix the coupling constants entering the calculation. For our  $\mathcal{O}(\epsilon^3)$  calculation it is appropriate to use  $F_\pi = 92.5$  MeV,  $M_N = 938$  MeV,  $\delta = 293$  MeV,  $m_\pi = 140$  MeV,  $g_A = 1.26$ ,  $g_{\pi N\Delta} = 1.05$  [19,37]. However, the four  $\gamma N\Delta$  couplings  $b_1, b_6, D_1, E_1$  as well as the leading  $\pi\Delta\Delta$  coupling  $g_1$  are only poorly known at the moment. Until we have more information on these couplings we therefore proceed *semiempirically* and evaluate the *exact*  $\mathcal{O}(\epsilon^3)$  SSE results of Secs. II–VI with phenomenological input from other calculations.

In particular, for the leading  $M1$  coupling we use  $b_1$

<sup>12</sup>The analogous phenomenon occurs for the slope parameters of the  $G_i(q^2)$ ,  $i=1,2,3$ , which we discuss in Sec. VII C.

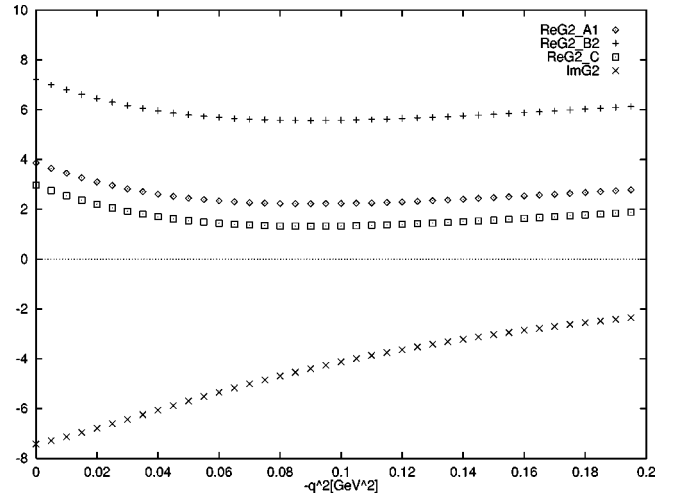


FIG. 3. The real and imaginary parts of the form factor  $G_2$  with  $C_2, C_3$  given by the sets  $A_1, B_2, C$ .

$=7.7$  as in Ref. [37],<sup>13</sup> although this is not entirely consistent with our  $\mathcal{O}(\epsilon^3)$  calculation as this particular strength for the coupling only holds to  $\mathcal{O}(\epsilon^2)$  and undergoes an as yet undetermined renormalization in  $\mathcal{O}(\epsilon^3)$ . The remaining three  $\gamma N\Delta$  couplings are still undetermined [21]; for now we find that we can parametrize them via *two independent linear combinations*  $C_2, C_3$  and fix them from Refs. [3,40] in the next section. Finally, as a result of a lack of more precise information at the moment, we use the SU(6) quark model estimate  $g_1 = \frac{9}{5}g_A$  for the  $\pi\Delta\Delta$  coupling in Eq. (17), which should be accurate to 25% (e.g., [41]). We also note that the so-called off-shell parameters  $y_{1,6}$  of Eq. (18) decouple from our results.

### A. Best estimate for unknown couplings

First, we note that the unknown couplings<sup>14</sup>  $b_6, D_1, E_1$  only show up via two independent linear combinations in our calculation. We therefore introduce the new set of parameters

$$C_2 \equiv \frac{2\bar{E}_1 - \bar{D}_1}{4}, \quad C_3 \equiv \frac{2b_6 - \bar{D}_1}{4}. \quad (46)$$

We now want to utilize existing phenomenological analyses for  $N\Delta$  transition multipoles in order to fix these two parameters. Most of the existing work relies on parametrizations of pion photoproduction in the delta region and has focused on the determination of the transition multipoles at the so called

<sup>13</sup>The factor of 2 difference compared to Ref. [37] just results from the fact that we use a different form for the  $\mathcal{O}(\epsilon^2)$   $\gamma N\Delta$  vertex in Eq. (19), in order to be consistent with the SSE formalism in paper [16]. The sign of  $b_1$  is chosen to give a positive result for the  $\mathcal{O}(\epsilon^2)$   $M1$   $\gamma N\Delta$  transition multipole at  $q^2=0$ , consistent with the previous analyses [2,3].

<sup>14</sup>For the numerical analysis we utilize the scale-independent couplings  $\bar{D}_1, \bar{E}_1$ .

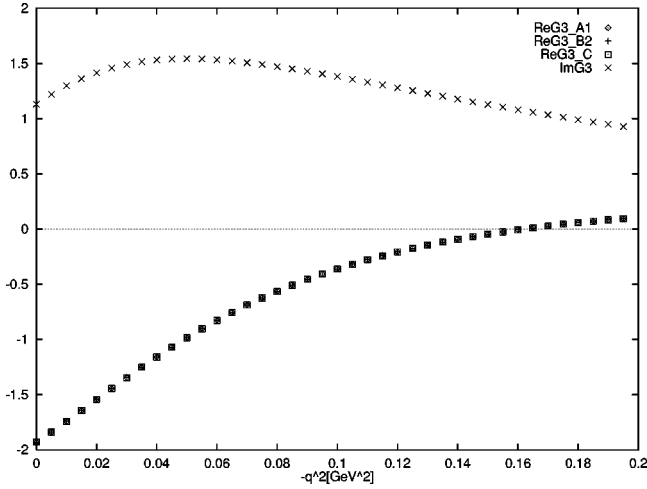


FIG. 4. The real and imaginary parts of the form factor  $G3$  with  $C_2, C_3$  given by the sets  $A_1, B_2, C$ .

$K$ -matrix pole position; e.g., see [2]. Unfortunately, this wealth of information is not directly transferable to our problem because the  $K$ -matrix approach by construction only gives the imaginary part of the transition amplitude at the kinematical point where the real part vanishes. For our calculation, however, we need information on the transition multipoles at the  $T$ -matrix pole, where  $M1, E2, C2$  can be complex quantities even at the resonance position. This information has recently become available [3,39,40]. Our fitting procedure will refer to either the values of the real part of the transition multipoles  $M1, E2$  at  $q^2=0$  or to the ratio  $E2/M1$  at  $q^2=0$ . We shall adopt the first choice for the RPI, VPI results [40] and the second one for the Mainz results [3]. The two parameter sets determined by fitting to  $\text{Re } M1(0)$ ,  $\text{Re } E2(0)$ , with  $\text{Re}$  denoting the real part, of the RPI, VPI data will be designated  $A$  and  $B$ , respectively, while a further subscript taking the values 1 or 2 will denote the two fits used in reference [40]. Specifically, using  $\text{Re } M1(0)=0.3 \text{ GeV}^{-1/2}$ ,  $\text{Re } E2(0)=-0.0087 \text{ GeV}^{-1/2}$  we obtain

$$\begin{aligned} C_2^A &= -7.80, \\ C_3^A &= -2.48, \end{aligned} \quad (47)$$

while using  $\text{Re } M1(0)=0.301 \text{ GeV}^{-1/2}$ ,  $\text{Re } E2(0)=-0.048 \text{ GeV}^{-1/2}$  we find

$$\begin{aligned} C_2^A &= -8.07, \\ C_3^A &= -2.91. \end{aligned} \quad (48)$$

We now consider the VPI group results. The values  $\text{Re } M1(0)=0.297 \text{ GeV}^{-1/2}$ ,  $\text{Re } E2(0)=0.0065 \text{ GeV}^{-1/2}$  give

$$C_2^B = -7.76,$$

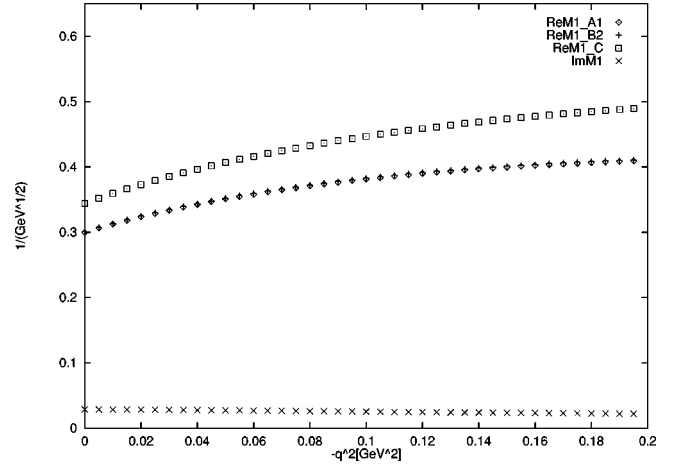


FIG. 5. The real and imaginary parts of the form factor  $M1$  with  $C_2, C_3$  given by the sets  $A_1, B_2, C$ .

$$C_3^B = -2.72, \quad (49)$$

and finally the values  $\text{Re } M1(0)=0.301 \text{ GeV}^{-1/2}$ ,  $\text{Re } E2(0)=-0.0011 \text{ GeV}^{-1/2}$  produce

$$\begin{aligned} C_2^B &= -8.27, \\ C_3^B &= -3.31. \end{aligned} \quad (50)$$

The next step is to use the speed-plot analysis<sup>15</sup> of the Mainz group [3]. This time we need our expression

$$\text{EMR}(0) \equiv \frac{E2(0)}{M1(0)} = \frac{\delta b_1 + \delta G_2(0)}{8M_N G_1(0) - \delta G_2(0)} \quad (51)$$

from Eq. (45) and Table I. We end up with a new parameter set, denoted by  $C$ :

$$\begin{aligned} \text{EMR}(0)_{\text{Mainz}} &= (-3.5 - 4.6i)\% \rightarrow C_2^C = -10.14 \\ &\rightarrow C_3^C = -2.25. \end{aligned} \quad (52)$$

All the fits produce ‘‘natural size’’ values for the parameters  $C_2, C_3$ . Based on the above parameter sets we may determine an average value and a relevant error for  $C_2, C_3$ . We arrive at the values

$$\begin{aligned} C_2 &= -8.41 \pm 0.44, \\ C_3 &= -2.73 \pm 0.18. \end{aligned} \quad (53)$$

<sup>15</sup>In view of the preliminary character of these numerical estimates we neglect the fact that the Mainz numbers were obtained at a pole position which would correspond to a smaller value for the nucleon-delta mass splitting parameter  $\delta$ .

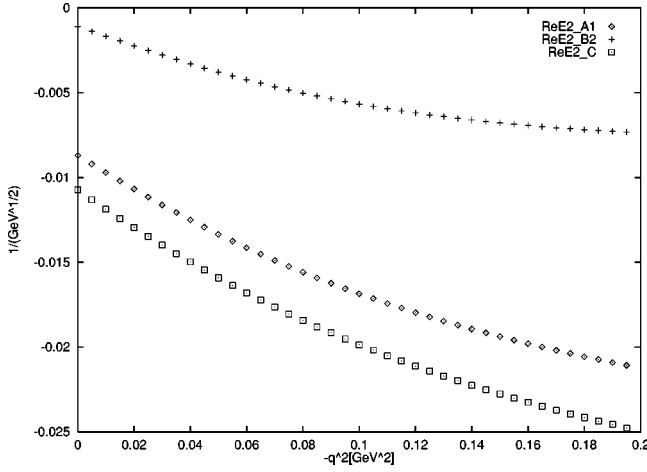


FIG. 6. The real part of the form factor  $E2$  with  $C_2, C_3$  given by the sets  $A_1, B_2, C$ .

### B. Predictions for the multipoles, CMR(0) ratio

Having fixed  $C_2, C_3$  in the previous subsection we can now give the following predictions for the average values of the electromagnetic form factors and their relevant errors:

$$\begin{aligned} M1(0) &= (308.6 \pm 8.9 + i28.6) \times 10^{-3} \text{ GeV}^{-1/2}, \\ E2(0) &= (-6.4 \pm 1.7 - i16.9) \times 10^{-3} \text{ GeV}^{-1/2}, \\ C2(0) &= (-10.8 \pm 1.7 - i14.3) \times 10^{-3} \text{ GeV}^{-1/2}. \end{aligned} \quad (54)$$

For the ratios we determine

$$\text{Re EMR}(0) \equiv \text{Re} \frac{E2(0)}{M1(0)} = (-2.52 \pm 0.48) \%, \quad (55)$$

$$\text{Im EMR}(0) \equiv \text{Im} \frac{E2(0)}{M1(0)} = (-5.24 \pm 0.16) \%, \quad (56)$$

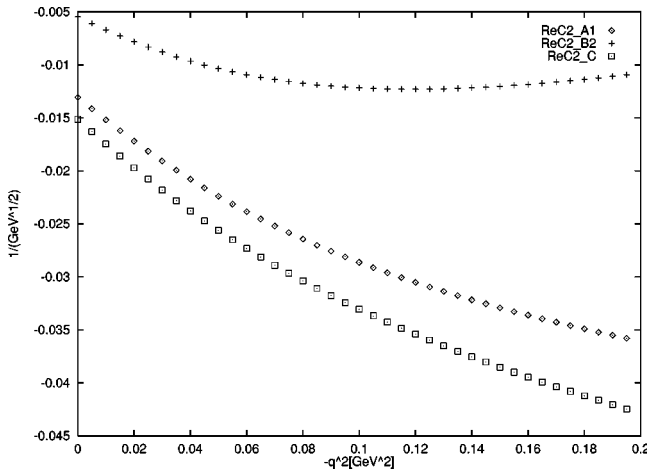


FIG. 7. The real part of the form factor  $C2$  with  $C_2, C_3$  given by the sets  $A_1, B_2, C$ .

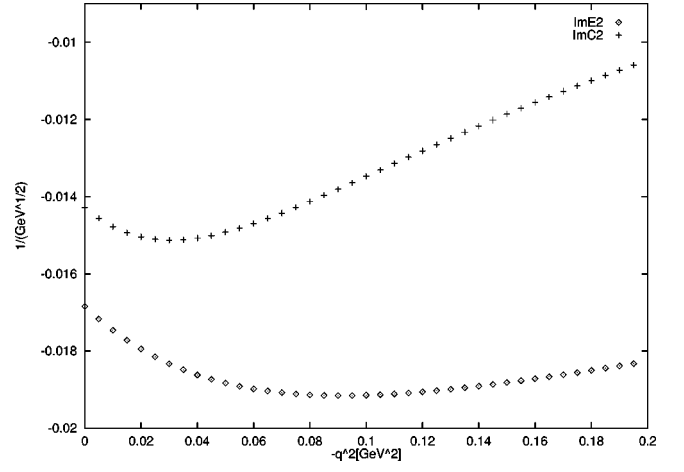


FIG. 8. The imaginary part of the form factors  $E2, C2$  with  $C_2, C_3$  given by the sets  $A_1, B_2, C$ .

$$\text{Re CMR}(0) \equiv \text{Re} \frac{C2(0)}{M1(0)} = (-3.86 \pm 0.47) \%, \quad (57)$$

$$\text{Im CMR}(0) \equiv \text{Im} \frac{C2(0)}{M1(0)} = (-4.29 \pm 0.14) \%. \quad (58)$$

We note that the imaginary parts of the multipole form factors (as well as the imaginary parts of the form factors  $G_i, i \in \{1, 2, 3\}$ ) are the same for all fits and so we are not in a position to produce error bars for them. The reason is simply that the imaginary part of the transition amplitude stems exclusively from loop contributions which do not depend on  $C_2, C_3$ . Of course the same is not true for the ratios of the multipoles since in this case real and imaginary parts of the numerator and the denominator are mixed in order to obtain the real and imaginary part of the ratio. We also note that our results appear much less sensitive to  $C_2$  compared with their dependence on  $C_3$ . The reason is that this first parameter appears only in the  $G_1$  form factor and its contribution with respect to the other ones is suppressed by a power of the ratio  $\delta/M_N$ .

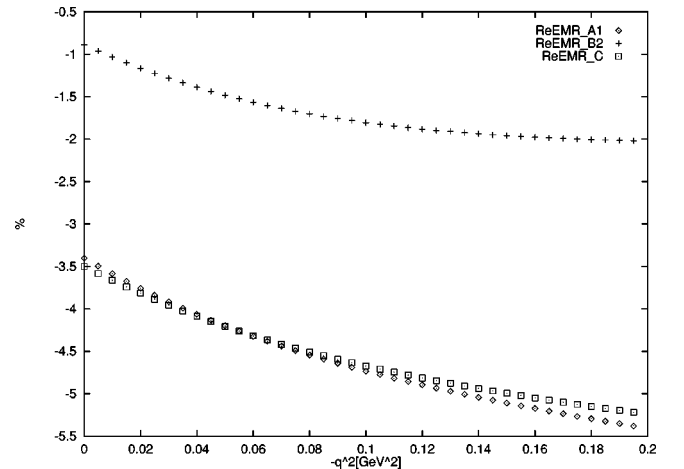


FIG. 9. The real part of the EMR ratio with  $C_2, C_3$  given by the sets  $A_1, B_2, C$ .



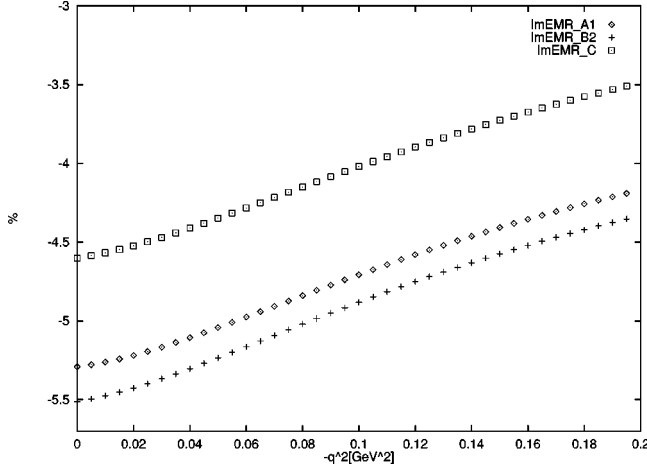


FIG. 10. The imaginary part of the EMR ratio with  $C_2, C_3$  given by the sets  $A_1, B_2, C$ .

In Figs. 2, 3, 4 the  $q^2$  dependence of both the real and the imaginary parts of  $G_1$ ,  $G_2$ , and  $G_3$  is depicted, using the  $C$ ,  $A_1$ , and  $B_2$  sets, respectively, for the values of the parameters  $C_2$ ,  $C_3$ . As for the real part of the form factor  $G_3$  we do not want to imply that it changes its sign near  $-q^2 = 0.15 \text{ GeV}^2$ . Given that  $G_3(q^2)$  approaches quickly to zero even small corrections from higher orders can change the result for  $-q^2 > 0.1 \text{ GeV}^2$ . The resulting  $q^2$  dependence of the multipole form factors  $M1$ ,  $E2$ ,  $C2$  is shown in Figs. 5, 6, 7, and 8. Finally the last remaining figures (Figs. 9, 10, 11, 12) show the real and the imaginary parts of the ratios EMR, CMR. We close the present section with a remark concerning the range of  $q^2$ , for which we believe our results to be meaningful. As we have already mentioned in the previous paragraph, the *imaginary* part of the amplitudes is determined entirely by a one-loop diagram related to  $\pi N$  scattering at the relatively large kinematic energy of approximately  $\delta - m_\pi \sim 150 \text{ MeV}$ . We therefore do not necessarily expect that the  $\mathcal{O}(\epsilon^3)$  calculation will lead to a good description of the *imaginary parts* and point to the *possibility* of large higher order corrections in the *imaginary parts* of the  $G_i(q^2)$

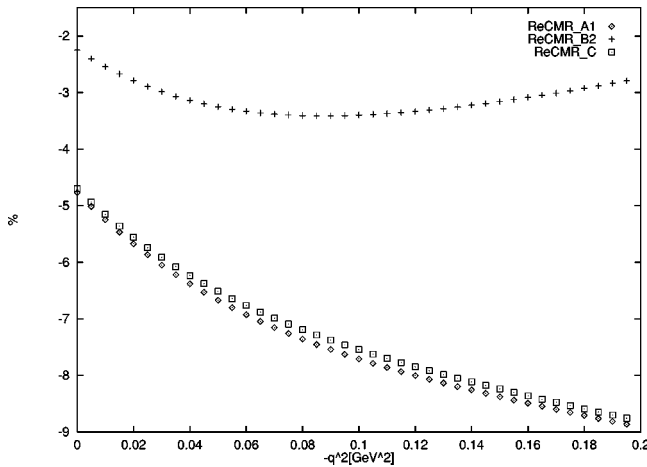


FIG. 11. The real part of the CMR ratio with  $C_2, C_3$  given by the sets  $A_1, B_2, C$ .

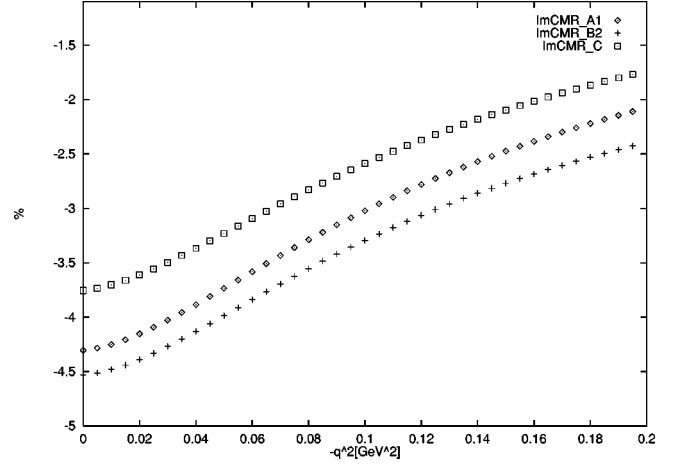


FIG. 12. The imaginary part of the CMR ratio with  $C_2, C_3$  given by the sets  $A_1, B_2, C$ .

form factors. This issue can only be resolved by a future  $\mathcal{O}(\epsilon^4)$  calculation.

### C. Predictions for the form factors

Though enjoying less fame than the corresponding transition multipoles of the previous section, the three  $N\Delta$  transition form factors  $G_i(q^2)$  are actually better suited for a chiral analysis—the reason being that to  $\mathcal{O}(\epsilon^3)$  the complete  $q^2$  dependence is solely governed by  $\mathcal{O}(\epsilon)$  parameters, whereas the poorly known couplings  $b_1, b_6, D_1, E_1$  only enter in the  $q^2=0$  normalization of the form factors. Utilizing  $C_2, C_3$  from the previous section one fixes

$$G_1(0) = (5.50 \pm 0.14 + i0.20),$$

$$G_2(0) = (4.90 \pm 0.73 - i7.42),$$

$$G_3(0) = (-1.93 + i1.13). \quad (59)$$

We note that all three imaginary parts and the real part of  $G_3(0)$  do not depend on the couplings  $b_1, b_6, D_1, E_1$  and are given by the much better known leading order parameters of SSE.

We now proceed to give predictions for the slope parameters<sup>16</sup>

$$\rho_i^2 \equiv 6 \frac{dG_i}{dt} \Big|_{t=0}, \quad (60)$$

which can be directly calculated from Eqs. (42)–(44). Defining  $\mu \equiv m_\pi / \delta$  and  $\mathcal{N} = -3g_{\pi N \Delta} g_A M_N / 4\pi^2 F_\pi^2 \delta$  we find

<sup>16</sup>We focus on the slope parameters rather than on the transition radii in order to avoid the appearance of any of the poorly known couplings  $b_1, b_6, D_1, E_1$  in the discussion.

$$\begin{aligned}
\rho_1^2 = & \mathcal{N} \left[ -\frac{3}{2} + 2\mu\pi - \frac{i}{3}\sqrt{-1+\mu^{-2}}\mu\pi + \frac{2}{3}\mu^3\pi - \frac{5}{8}\mu^2\pi^2 + \frac{\mu}{3}\sqrt{-1+\mu^{-2}}\log\left(-\sqrt{-1+\mu^{-2}} + \frac{1}{\mu}\right) \right. \\
& + \frac{2}{3}\mu^3\sqrt{-1+\mu^{-2}}\log\left(-\sqrt{-1+\mu^{-2}} + \frac{1}{\mu}\right) + \frac{\mu^2}{2}\log^2\left(-\sqrt{-1+\mu^{-2}} + \frac{1}{\mu}\right) + \frac{4}{3}\mu\sqrt{-1+\mu^{-2}}\log\left(\sqrt{-1+\mu^{-2}} + \frac{1}{\mu}\right) \\
& + \frac{2}{3}\sqrt{-1+\mu^{-2}}\mu^3\log\left(\sqrt{-1+\mu^{-2}} + \frac{1}{\mu}\right) - \frac{2}{3}i\sqrt{-1+\mu^{-2}}\mu^3\pi + i\mu^2\pi\log\left(\sqrt{-1+\mu^{-2}} + \frac{1}{\mu}\right) \\
& \left. - \mu^2\log^2\left(\sqrt{-1+\mu^{-2}} + \frac{1}{\mu}\right) \right]. \tag{61}
\end{aligned}$$

One can see immediately that  $\rho_1^2$  is suppressed by a power of  $1/\Lambda_\chi \approx 1/M_N$  compared to the real photon point  $q^2=0$ . This behavior can also be observed in the  $F_2(q^2)$  Dirac form factor of the nucleon (e.g., [17,19]). An analogous result is expected for the radius of the  $M1(q^2)$  form factor; see the discussion in Sec. VI.

For the slope parameters corresponding to  $G_2$  and  $G_3$ ,  $t$  differentiation of the  $J$ ,  $H$  functions is needed, resulting in two divergent contributions (one nonintegrable singularity resulting from differentiating under the integral sign and one divergent surface term from differentiating with respect to the integration limit). Treating the integral as a principal-valued one the infinities are shown to cancel out, leaving

$$\begin{aligned}
\rho_2^2 = & 4\pi\mathcal{N}\frac{M_N}{\delta} \left\{ 2\mu - \frac{3}{2}\pi\mu^2 + \frac{8}{3}\mu^3 - i \left[ \sqrt{1-\mu^2} \left( \frac{1+8\mu^2}{3} \right) \right. \right. \\
& \left. \left. - 3\mu^2 \log\left(\frac{1}{\mu} + \sqrt{\frac{1}{\mu^2}-1}\right) \right] \right\}, \\
\rho_3^2 = & -2\pi\mathcal{N}\frac{M_N}{\delta} \left\{ 8\mu + \frac{16}{3}\mu^3 - \left( 1 + \frac{15}{2}\mu^2 \right) \right. \\
& \times \left[ \frac{\pi}{2} - i \log\left(\frac{1}{\mu} + \sqrt{\frac{1}{\mu^2}-1}\right) \right] \\
& \left. - i\sqrt{1-\mu^2} \left( \frac{19}{6} + \frac{16}{3}\mu^2 \right) \right\}. \tag{62}
\end{aligned}$$

It is important to note that this is a quite peculiar result. One can see immediately that these two slope parameters<sup>17</sup> scale as  $\Lambda_\chi^0 \approx M_N^0$ ; i.e., they show no suppression by a heavy scale with respect to the  $q^2=0$  point. This behavior is completely analogous to the one expected for  $E2(q^2)$ ,  $C2(q^2)$  (cf. Sec. VI), but has not yet been observed in chiral calculations of baryon form factors. The first moment with respect to  $q^2$  of these ‘‘quadrupolelike’’ form factors  $G_2(q^2)$ ,  $G_3(q^2)$  is entirely given by the small scales  $m_\pi$ ,  $\delta$  and leading order coupling constants—allowing, *in principle*, a large variation of the form factors at low  $q^2$  compared to their  $q^2=0$  point.

<sup>17</sup>The same of course holds for the corresponding transition radii.

However, we want to emphasize that Eqs. (61),(62) only represent the leading results for the three slope parameters; more cannot be learned from a  $\mathcal{O}(\epsilon^3)$  calculation. At present, we have no way of knowing the size of the  $\mathcal{O}(\epsilon^4)$  corrections, but in principle it is possible to calculate them at a later stage.<sup>18</sup>

Finally, we can obtain the chiral limit ( $\mu \rightarrow 0$ ) behavior of the slope parameters from Eqs. (61, 62),

$$\begin{aligned}
\rho_1^2 = & \mathcal{N} \left[ -\frac{3}{2} - \frac{i\pi}{3} + \log 2 - \log \mu \right] + \mathcal{O}(\mu), \\
\rho_2^2 = & -\frac{4}{3}i\pi\mathcal{N}\frac{M_N}{\delta} + \mathcal{O}(\mu), \\
\rho_3^2 = & -2\pi\mathcal{N}\frac{M_N}{\delta} \left[ -\frac{\pi}{2} + i \left( \log 2 - \log \mu - \frac{19}{6} \right) \right] \\
& + \mathcal{O}(\mu). \tag{63}
\end{aligned}$$

Thus, the real part of  $\rho_1^2$  diverges logarithmically in the chiral limit while its imaginary part remains finite. On the other hand, the real part of  $\rho_2^2$  vanishes altogether in the chiral limit, while its imaginary part remains finite. As for  $\rho_3^2$ , it is the real part that remains finite in the chiral limit while its imaginary part diverges logarithmically. The numerical values for the slope parameters are also collected in Table II and, since they take contributions only from the loops, are independent from the values of  $C_2$ ,  $C_3$ .

## VIII. SUMMARY AND OUTLOOK

The main features of our investigation can be summarized as follows.

The  $\Delta \rightarrow N\gamma^*$  amplitude has been calculated to  $\mathcal{O}(\epsilon^3)$  in the ‘‘small scale expansion’’ formalism. The pertinent counterterm contributions, relevant  $1/M$  corrections to lower order coupling, and all loop diagrams allowed to this order have been analyzed systematically. It was found that the  $q^2$

<sup>18</sup>At first one would need a precise determination of  $b_1$  and the subleading corrections to the  $\pi N\Delta$  vertex, as these couplings would enter the new loop diagrams of  $\mathcal{O}(\epsilon^4)$ .

TABLE II. The slope parameters [fm<sup>2</sup>] of the form factors  $G_i(q^2)$ .

$\rho_1^2$	$\rho_2^2$	$\rho_3^2$
1.94+0.55i	10.50−6.16i	−4.12−4.48i

dependence of the transition is generated by two  $\pi N$ -,  $\pi\Delta$ -loop diagrams and that two counterterms are needed to renormalize the result.

We have obtained an estimate for presently poorly known couplings from existing phenomenological analyses and then given predictions for the complex transition multipoles  $M1(q^2)$ ,  $E2(q^2)$ ,  $C2(q^2)$  as well as the complex multipole ratios  $\text{CMR}(0)$ ,  $\text{EMR}(q^2)$ ,  $\text{CMR}(q^2)$ . While matching the  $\mathcal{O}(\epsilon^3)$  results to the corresponding expressions of the multipoles as functions of  $q^2$  we found that the radii of the quadrupole form factors are not suppressed by a large scale compared to the  $q^2=0$  point, indicating a possibly rapid variation at low  $q^2$ . Further study of this interesting result will continue once more precise information on the necessary couplings is available.

Three appropriately defined electromagnetic  $N\Delta$  transition form factors  $G_i(q^2)$ ,  $i=1,2,3$ , have been identified from the  $\mathcal{O}(\epsilon^3)$   $\Delta \rightarrow N\gamma^*$  calculation. The longitudinal form factor  $G_3(q^2)$  had to be rescaled compared to existing definitions in the literature in order to achieve consistency with the power counting of SSE.  $G_1(q^2)$  could be found to sub-leading order, whereas for  $G_2(q^2), G_3(q^2)$  we obtained the leading result.

The three  $G_i(q^2)$  form factors are found to be complex quantities due to the  $\pi N$ -loop diagram (i) in Fig. 1. Their entire  $q^2$  dependence is controlled by relatively well-known  $\mathcal{O}(\epsilon)$  parameters—making the  $G_i(q^2)$  form factors the preferred testing ground of chiral symmetry in the radiative  $N\Delta$  transition. The corresponding slope parameters have been calculated and their chiral limit behavior has been discussed.

The numerical results of this work have to be considered preliminary due to the presently poor state of knowledge on coupling constants in the SSE formalism. However, this situation is going to improve in the near future and we will at a later point revisit our  $\mathcal{O}(\epsilon^3)$  analytical results and try to improve upon the numerical accuracy of our predictions.

### ACKNOWLEDGMENTS

We would like to thank V. Bernard, R. Davidson, U.-G. Meissner, M. Neubert, C.N. Papanicolas, and R. Workman for valuable discussions. C.N.K. also wishes to acknowledge several interesting exchanges with A. Bernstein. The research of C.N.K. and G.C.G. has been supported in part by the EU Programme ‘‘Training and Mobility of Researchers,’’ Network ‘‘Hadronic Physics with High Energy Electromagnetic probes,’’ Contract No. ERB FMRX-CT96-0008. Finally, the research of G.P. has been financed through Grant No. ERBFMBICT 961491. T.R.H. would like to thank the National Institute for Nuclear Theory (INT) in Seattle for its hospitality, where part of this work was done.

### APPENDIX: INTEGRALS

The  $A^{ijk}(\Omega, M_t^2)$  functions used in Eq. (36) are defined as Euclidean integrals in dimensional regularization:

$$A^{ijk}(\Omega, M_t^2) \equiv \int_0^\infty \alpha^j d\alpha \int \frac{d^d l_E}{(2\pi)^d} \frac{(-l_E^2)^k}{\left(-l_E^2 - \frac{1}{4}\alpha^2 + \alpha\Omega - M_t^2\right)^i}. \quad (\text{A1})$$

To calculate them, first of all, we express the denominator using the Schwinger proper time representation:

$$\int_0^\infty dx x^{n-1} e^{-Ax} = \frac{\Gamma(n)}{A^n}, \quad A > 0, \quad (\text{A2})$$

with  $\Gamma(n)$  the well-known  $\Gamma$  function. The constraint  $A > 0$  is explicitly satisfied for the  $\Omega < 0$  case while for  $\Omega > 0$  we analytically continue our expressions. Finally using the tabulated integrals

$$\int_0^\infty x^{\nu-1} e^{-\beta x^2 - \gamma x} dx = (2\beta)^{-(\nu/2)} \Gamma(\nu) \exp\left(\frac{\gamma^2}{8\beta}\right) D_{-\nu}\left(\frac{\gamma}{(2\beta)^{1/2}}\right), \quad (\text{A3})$$

$$\begin{aligned} & \int_0^\infty e^{-zt} t^{-1+\beta/2} D_{-\nu}[2(kt)^{1/2}] dt \\ &= \frac{2^{1-\beta-\nu/2} \Gamma(\beta)}{\Gamma\left(\frac{1}{2}\nu + \frac{1}{2}\beta + \frac{1}{2}\right)} (z+k)^{-\beta/2} \\ & \quad \times F\left(\frac{\nu}{2}, \frac{\beta}{2}; \frac{\nu+\beta+1}{2}; \frac{z-k}{z+k}\right), \quad (\text{A4}) \end{aligned}$$

with  $D_{-\nu}(x)$  the parabolic cylinder function and  $F(a, b; c; x)$  the hypergeometric function, we find, explicitly,

$$\begin{aligned} \frac{A^{301}}{d} &= -L\Omega + \frac{\Omega}{32\pi^2} \left(1 - \ln \frac{M_t^2}{\mu^2}\right) + \frac{1}{16\pi^2} \\ & \quad \times \begin{cases} -\sqrt{M_t^2 - \Omega^2} \arccos\left(-\frac{\Omega}{M_t}\right), \\ +\sqrt{\Omega^2 - M_t^2} \ln\left(-\frac{\Omega}{M_t} + \sqrt{\frac{\Omega^2}{M_t^2} - 1}\right), \end{cases} \\ \frac{A^{301}}{d(d-1)} &= -\frac{1}{3}L\Omega + \frac{\Omega}{288\pi^2} \left(5 - 3 \ln \frac{M_t^2}{\mu^2}\right) + \frac{1}{48\pi^2} \\ & \quad \times \begin{cases} -\sqrt{M_t^2 - \Omega^2} \arccos\left(-\frac{\Omega}{M_t}\right), \\ +\sqrt{\Omega^2 - M_t^2} \ln\left(-\frac{\Omega}{M_t} + \sqrt{\frac{\Omega^2}{M_t^2} - 1}\right), \end{cases} \end{aligned}$$

$$\begin{aligned}
A^{310} &= 2L + \frac{1}{16\pi^2} \left( 1 + \ln \frac{M_t^2}{\mu^2} \right) - \frac{\Omega}{8\pi^2} \\
&\quad \times \begin{cases} \frac{1}{\sqrt{M_t^2 - \Omega^2}} \arccos \left( -\frac{\Omega}{M_t} \right), \\ \frac{1}{\sqrt{\Omega^2 - M_t^2}} \ln \left( -\frac{\Omega}{M_t} + \sqrt{\frac{\Omega^2}{M_t^2} - 1} \right), \end{cases} \\
\frac{d-3}{d-1} A^{310} &= \frac{2}{3} L + \frac{1}{144\pi^2} \left( 7 + 3 \ln \frac{M_t^2}{\mu^2} \right) - \frac{\Omega}{24\pi^2} \\
&\quad \times \begin{cases} \frac{1}{\sqrt{M_t^2 - \Omega^2}} \arccos \left( -\frac{\Omega}{M_t} \right), \\ \frac{1}{\sqrt{\Omega^2 - M_t^2}} \ln \left( -\frac{\Omega}{M_t} + \sqrt{\frac{\Omega^2}{M_t^2} - 1} \right), \end{cases} \\
A^{300} &= -\frac{1}{16\pi^2} \\
&\quad \times \begin{cases} \frac{1}{\sqrt{M_t^2 - \Omega^2}} \arccos \left( -\frac{\Omega}{M_t} \right), \\ \frac{1}{\sqrt{\Omega^2 - M_t^2}} \ln \left( -\frac{\Omega}{M_t} + \sqrt{\frac{\Omega^2}{M_t^2} - 1} \right), \end{cases} \\
\frac{d-3}{d-1} A^{300} &= \frac{1}{3} A^{300}, \tag{A5}
\end{aligned}$$

where the factor  $L$  carries the infinity in dimensional regularization and is defined in Eq. (39). It is clear that  $A^{300}$  is

finite while  $A^{310}$  and  $A^{301}$  diverge. The integrals in Eq. (37) are split between  $[0, x_0]$  (trigonometric branch) and  $(x_0, 1]$  (logarithmic branch) where  $x_0$  is the large root of  $\Omega^2 = M_t^2$ ,

$$x_0 = \frac{-t + \sqrt{t^2 + 4m_\pi^2 |\mathbf{q}|^2}}{2|\mathbf{q}|^2},$$

with  $t = \delta^2 - |\mathbf{q}|^2$  to the order we work. In the calculation the functions are defined with  $\Omega = \delta x$  for the  $N\pi$  intermediate state loop diagram and  $\Omega = -\delta x$  for the  $\Delta\pi$  one. This entails [cf. Eq. (A5)] that the logarithms have negative arguments (and therefore there is an absorptive piece of the amplitude) for the  $N\pi$  diagram alone, as expected from general considerations [ $s = M_\Delta^2 \geq (M_t + m_\pi)^2$  for  $i = N$  only]. The imaginary parts are computed analytically.

For completeness, we show the correspondence between our  $A$  functions and the  $J$  functions appearing in the literature (e.g., [37]):

$$\begin{aligned}
A^{200}(\Omega, M_t^2) &= J_0(\Omega, M_t^2), \\
A^{201}(\Omega, M_t^2) &= dJ_2(\Omega, M_t^2), \\
A^{300}(\Omega, M_t^2) &= \frac{1}{2} \frac{\partial}{\partial M_t^2} J_0(\Omega, M_t^2), \\
A^{301}(\Omega, M_t^2) &= \frac{d}{2} \frac{\partial}{\partial M_t^2} J_2(\Omega, M_t^2), \\
A^{310}(\Omega, M_t^2) &= -\frac{1}{2} \frac{\partial}{\partial \Omega} J_2(\Omega, M_t^2) = \frac{\partial}{\partial M_t^2} J_1(\Omega, M_t^2). \tag{A6}
\end{aligned}$$

- 
- [1] R. Beck *et al.*, Phys. Rev. Lett. **78**, 606 (1997); G. Blanpied *et al.*, *ibid.* **79**, 4337 (1997); F. Kalleicher *et al.*, Z. Phys. A **359**, 201 (1997).
- [2] R. M. Davidson, N. C. Mukhopadhyay, and R. S. Wittman, Phys. Rev. D **43**, 71 (1991); R. A. Arndt, I. I. Strakovsky, and R. L. Workman, Phys. Rev. C **56**, 577 (1997).
- [3] O. Hanstein, D. Drechsel, and L. Tiator, Phys. Lett. B **385**, 45 (1996); Nucl. Phys. **A632**, 561 (1998).
- [4] P. Bartsch *et al.*, talk given at the Proceedings of Baryons 98; M. O. Distler *et al.*, *ibid.*; R. W. Gothe *et al.*, *ibid.*
- [5] C. M. Becchi and G. Morpurgo, Phys. Lett. **17B**, 352 (1965); N. Isgur and G. Karl, Phys. Rev. D **18**, 4187 (1978); N. Isgur *et al.*, *ibid.* **25**, 2394 (1982).
- [6] For example, see Proceedings of Joint ECT\*/Jefferson Lab Workshop on N\* Physics and Non-perturbative QCD, edited by V. Burkert *et al.*, Few Body Phys. (to be published).
- [7] Bates-OOPS Collaboration, C.N. Papanicolas, spokesperson; MAMI-A1 Collaboration, R. Neuhausen, spokesperson; ELSA-ELAN Collaboration, B. Schoch, spokesperson; BNL-LEGS Collaboration, A. Sandorfi, spokesperson.
- [8] C. M. Carlson and N. C. Mukhopadhyay, Phys. Rev. Lett. **81**, 2646 (1998).
- [9] G. Kälbermann and J. M. Eisenberg, Phys. Rev. D **28**, 71 (1984); K. Bermuth *et al.*, *ibid.* **37**, 89 (1988); D. Lu *et al.*, Phys. Rev. C **55**, 3108 (1997).
- [10] A. Buchmann, talk given at the Proceedings of Baryons 98 [4].
- [11] D. B. Leinweber *et al.*, Phys. Rev. D **48**, 2230 (1993).
- [12] M. N. Butler, M. J. Savage, and R. P. Springer, Phys. Lett. B **304**, 353 (1993).
- [13] M. Napsuciale and J. L. Lucio, Nucl. Phys. **B494**, 260 (1997).
- [14] R. L. Workman, talk given at the Proceedings of Baryons 98 [4].
- [15] T. R. Hemmert, B. R. Holstein, and J. Kambor, Phys. Lett. B **395**, 89 (1997).
- [16] T. R. Hemmert, B. R. Holstein, and J. Kambor, J. Phys. G **24**, 1831 (1998).
- [17] For example, V. Bernard, N. Kaiser, and U.-G. Meissner, Int. J. Mod. Phys. E **4**, 193 (1995).
- [18] T. R. Hemmert, Few-Body Syst. Suppl. **11**, 78 (1999).
- [19] V. Bernard, H. W. Fearing, T. R. Hemmert, and U.-G.

- Meissner, Nucl. Phys. **A635**, 121 (1998).
- [20] H. F. Jones and M. D. Scadron, Ann. Phys. (N.Y.) **81**, 1 (1973); R. C. E. Devensish, T. S. Eisenschitz, and J. G. Körner, Phys. Rev. D **14**, 3063 (1976); R. Davidson (private communication).
- [21] V. Bernard, T. R. Hemmert, and U.-G. Meissner, “The Role of  $\Delta(1232)$  in Pion Photoproduction” (in preparation).
- [22] S. Weinberg, Physica A **96**, 327 (1979).
- [23] J. Gasser and H. Leutwyler, Ann. Phys. (N.Y.) **158**, 142 (1984); Nucl. Phys. **B250**, 465 (1985).
- [24] N. Isgur and M. Wise, Phys. Lett. B **232**, 113 (1989); **237**, 527 (1990).
- [25] H. Georgi, Phys. Lett. B **240**, 447 (1990).
- [26] E. Jenkins and A. Manohar, Phys. Lett. B **255**, 558 (1991).
- [27] V. Bernard, J. Kambor, N. Kaiser, and U.-G. Meissner, Nucl. Phys. **B388**, 315 (1992).
- [28] E.g., M. Finkemeier, H. Georgi, and M. McIrvin, Phys. Rev. D **55**, 6933 (1997).
- [29] G. Ecker, hep-ph/9805500, 1998.
- [30] J. Gasser, M. E. Sainio, and A. Svarc, Nucl. Phys. **B307**, 779 (1988).
- [31] G. Ecker and M. Mojizis, Phys. Lett. B **365**, 312 (1996).
- [32] N. Fettes, U.-G. Meissner, and S. Steininger, Nucl. Phys. **A640**, 199 (1998).
- [33] U.-G. Meissner, G. Müller, and S. Steininger, hep-ph/9809446, 1998.
- [34] ChPT97, in *Chiral Dynamics*, Proceedings of the Workshop: Theory and Experiment, Mainz, Germany, 1997, edited by A. Bernstein, D. Drechsel, and T. Walcher (Springer Verlag, Heidelberg, 1998).
- [35] E. Jenkins and A. Manohar, Phys. Lett. B **259**, 353 (1991).
- [36] J. Kambor, in *Chiral Dynamics* [34].
- [37] T. R. Hemmert, B. R. Holstein, J. Kambor, and G. Knöchlein, Phys. Rev. D **57**, 5746 (1998); T. R. Hemmert, B. R. Holstein, and J. Kambor, *ibid.* **55**, 5598 (1997).
- [38] For example, see T. Ericson and W. Weise, *Pions and Nuclei* (Oxford Science Publications, Oxford, 1998).
- [39] R. L. Workman and R. A. Arndt, Phys. Rev. C **59**, 1810 (1999).
- [40] R. M. Davidson *et al.*, Phys. Rev. C **59**, 1059 (1999).
- [41] T. R. Hemmert, B. R. Holstein, and N. C. Mukhopadhyay, Phys. Rev. D **51**, 158 (1995).